

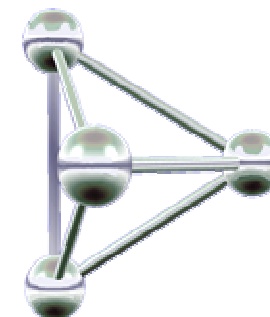
**Freiberg University of Mining and
Technology, Germany**



Thermodynamics of High Temperature Materials Systems

Hans Jürgen Seifert

**Summer School
Advanced Thermostructural Materials
Santa Barbara, August 9, 2006**



Thermodynamics of High Temperature Materials Systems

Hans Jürgen Seifert

Outline

1. Introduction and motivation for thermodynamic calculations

- Computational thermodynamics
- CALPHAD approach (CALculation of PHAse Diagrams)
- Thermodynamic databases and software

2. Thermodynamic optimization of the Ce-O system

- Thermodynamic modeling of solution phases

3. Precursor-derived Si-(B-)C-N ceramics

- High temperature reactions of silicon carbide and silicon nitride ceramics
 - Crystallization and high temperature stability of Si-(B-)C-N ceramics
-

Thermodynamics of High Temperature Materials Systems

Hans Jürgen Seifert

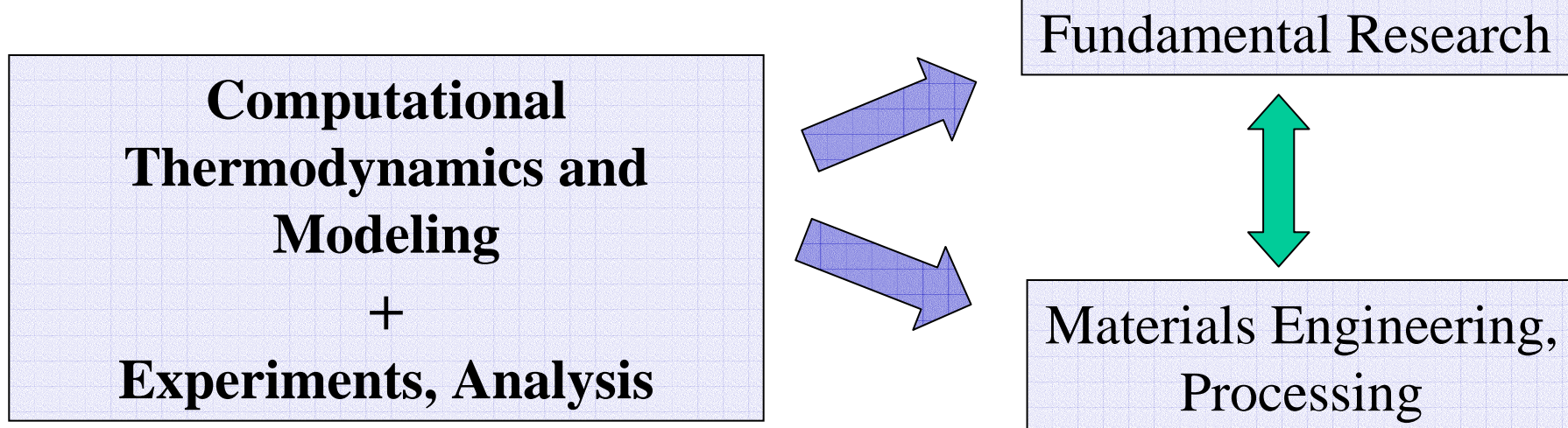
Outline

4. Computational thermodynamics in heat shield engineering

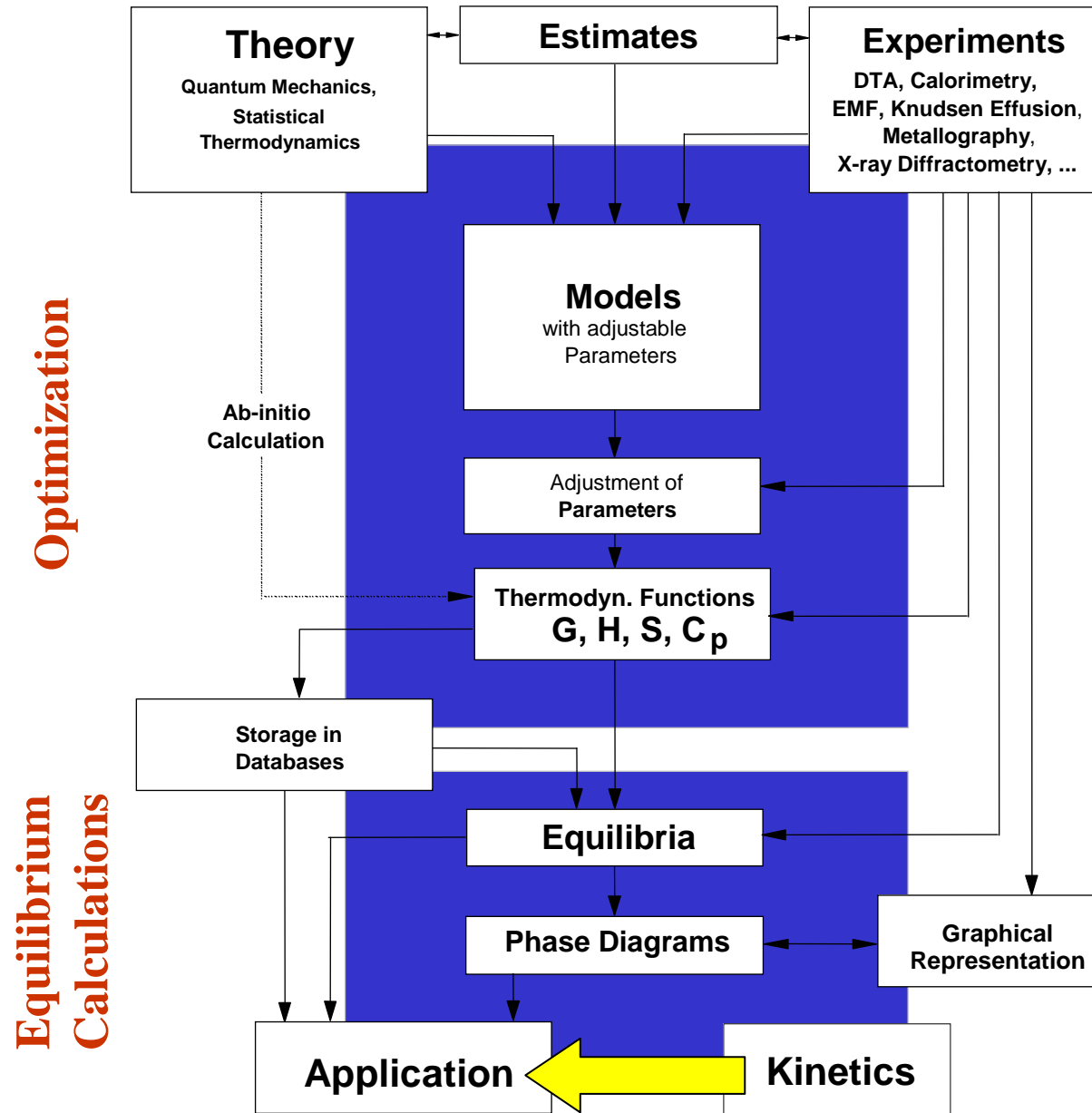
- The Y-Si-C-O system database
- Active / passive oxidation of SiC
- Phase reactions of Yttrium silicates and C/C-SiC composites
- High temperature stability issues in the engineering of heat shields

5. Conclusions

Combined Approach



Computational Thermodynamics



CALPHAD

CALculation
of PHase Diagrams

CALPHAD (CALculation of PHAse Diagrams)

- Development of Optimized Thermodynamic Datasets stored in Computer Databases
- Calculation of :
 - Thermodynamic Functions
 - Liquidus Surface
 - Isothermal Sections
 - Isopleths
 - Potential Phase Diagrams
 - Phase Fraction Diagrams
 - Phase Compositions
 - Scheil Solidification
 - ...

**Requires Modeling of Stoichiometric and Solution Phases
Taking into Account the (Crystal-) Structures and Site Occupancies**

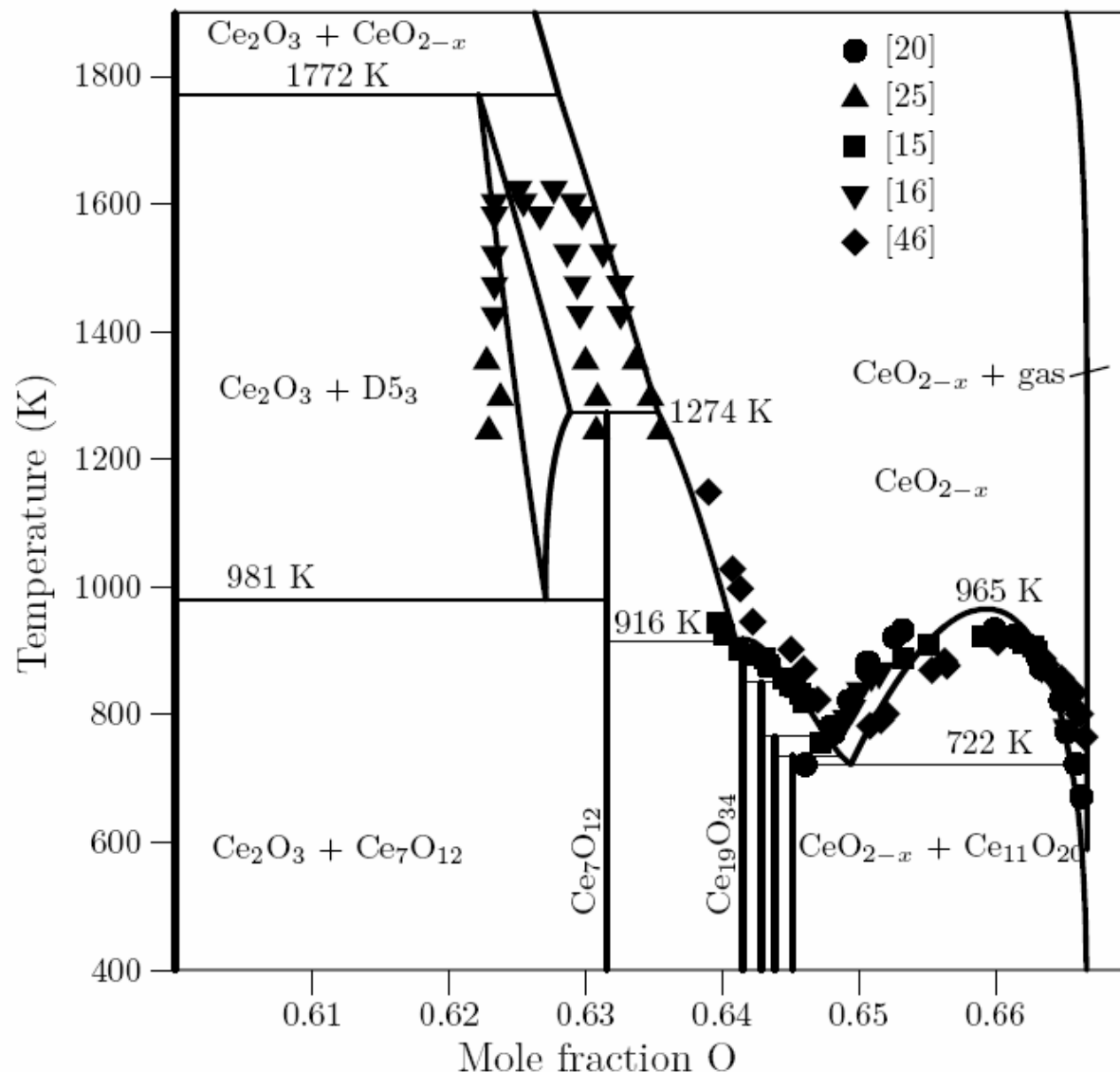
CALPHAD (CALculation of PHAse Diagrams) Software

- LUKAS (BINGSS, BINFKT, TERGSS, TERFKT)
- THERMO-CALC
- FACTSAGE
- PANDAT
- MALT, MALT2
- MTDATA
- JMATPRO
- GEMINI
- ...

CALPHAD (CALculation of PHAse Diagrams) Databases

- SGTE, Scientific Group Thermodata Europe
 - SSOL2, SSOL4
 - SSUB3
 - Noble Metals
- Thermo-Calc: Steels, Ni-base, slags, ...
- ThermoTech: Ni-base, Al-, Mg-, ...
- PML: Al-, Ceramics
- ...

Calculated Ce–O System in Solid State from 60 to 67 mol. % O in comparison with experimental data.

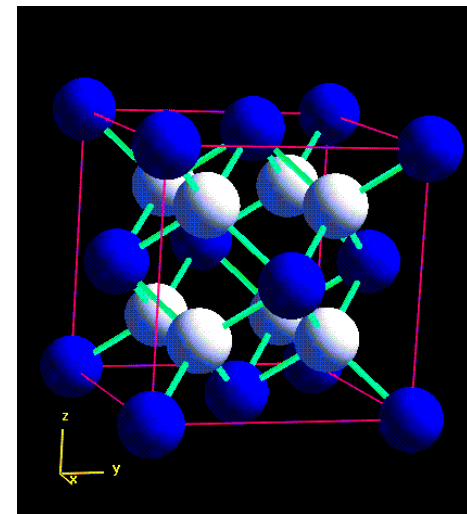
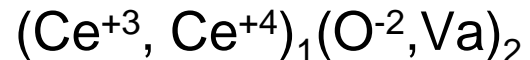


Phases in the Partial Ce – O System

Related Crystal Structures:

CeO_{2-x} (ss) CaF₂ - type (Strukturbericht C1)

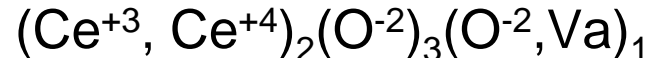
Compound Energy Formalism:



C-Ce₂O₃ (ss) Mn₂O₃ - type (Strukturbericht D5₃, Ordered State of C1)

Unit Cell: composed of 8 CaF₂-type cells. ¼ of O-ions removed, remaining atoms re-arrange towards these vacancies.

Compound Energy Formalism:



Contains more O atoms than the ideal formula of the Mn₂O₃.

Ce₂O₃ Stoichiometric phase description (Strukturbericht D5₂)

“Compound Energy” Formalisms – Reference Compounds

$(A,B)_k(D,E)_l$ *Solution phase with
two sublattices and 4 species*

Four compounds defined:

A : D

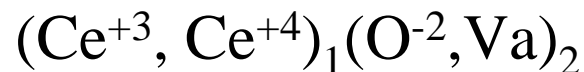
A : E

B : D

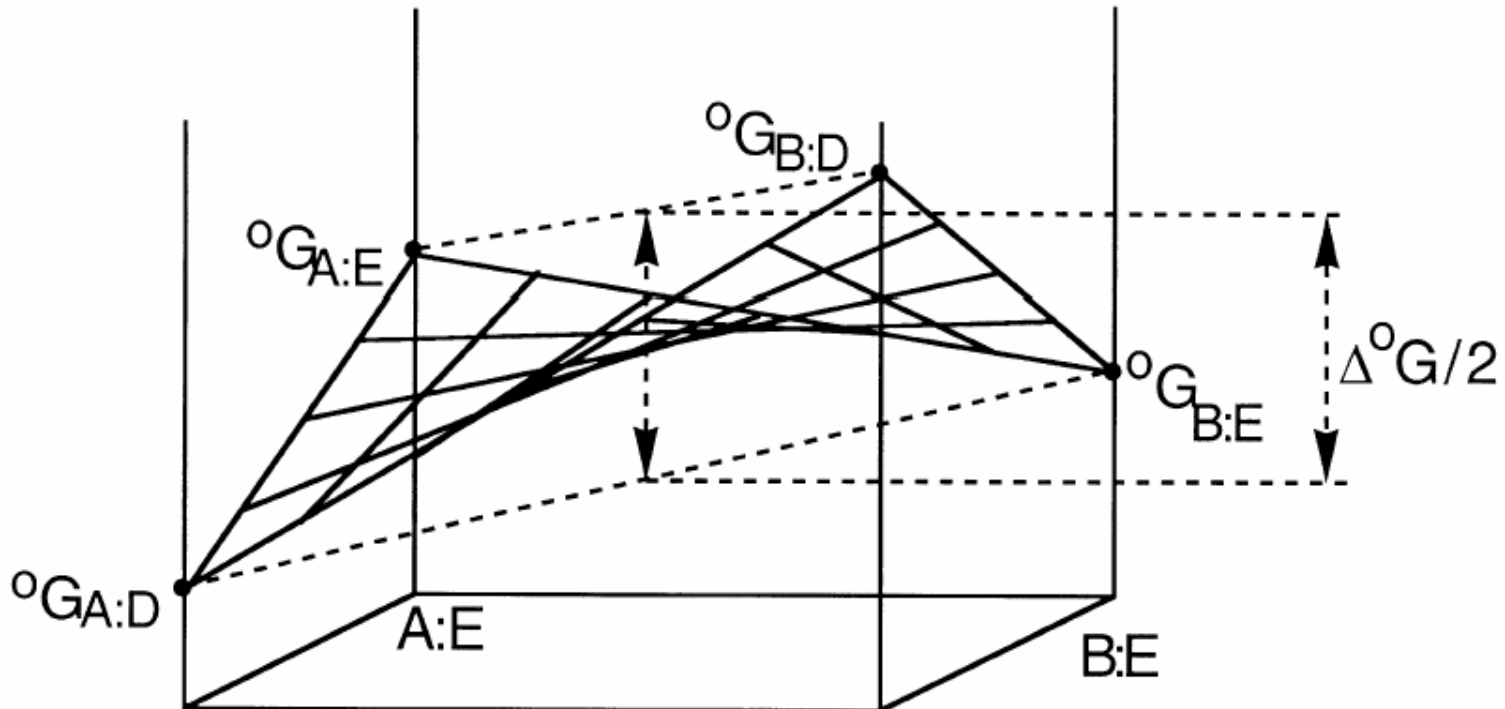
B : E

Gibbs free energy for every compound to be determined

Here:



“Compound Energy” Formalism – Surface of Reference



$$G_m^{\text{s.r.}} = \sum \circ G_{\text{end}} \prod y_J^S$$

$(A,B)_k(D,E)_l$

*Solution phase with
two sublattices and 4 species*

Modeling of solution phases; sublattice model described in the Compound Energy Formalism

$(A,B)_k(D,E)_l$

Solution phase with two sublattices and 4 species

$$-S_m^{\text{mix}}T = RT \sum\sum n^s y_J^s \ln(y_J^s)$$

n^s

Stoichiometric coefficient (s: sublattice)

y_A^s

Site fraction of species A on sublattice s

$$\sum y_J^s = 1$$

Compound Energy Formalism – Excess term of Gibbs free energy

(A,B)_k(D,E)_l *Solution phase with
two sublattices and 4 species*

$$\begin{aligned} {}^E G_m &= \prod y_J^s \sum y_B^t L_{A,B:D:G} \dots \\ &\quad + \prod y_J^s \sum \sum y_B^t y_D^u L_{A,B:D,E:G} \dots + \dots \end{aligned}$$

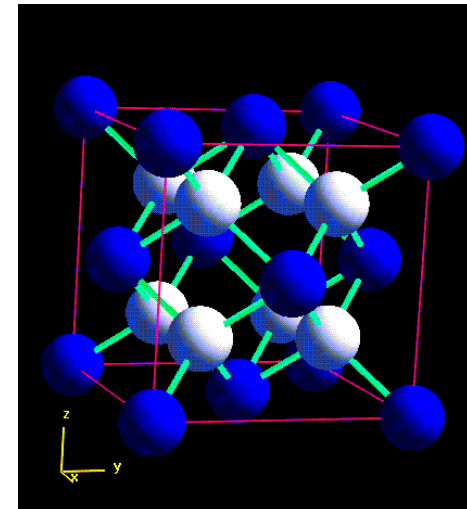
Compound Energy Formalisms – Gibbs free energy of solution phases

$$\begin{aligned} \text{Mixing Gibbs Energy} &= \sum \Delta_f^\circ G_{\text{end}} \Pi y_J^s \\ &+ RT \sum \sum n^s y_J^s \ln(y_J^s) + {}^E G_m. \end{aligned}$$

Phases in the Partial Ce – O System

CeO_{2-x} (ss) CaF_2 - type (Strukturbericht C1)

Compound Energy Formalism:
 $(\text{Ce}^{+3}, \text{Ce}^{+4})_1(\text{O}^{-2}, \text{Va})_2$



Cubic close pack of Ce ions, where all the tetrahedral voids form the sublattice on which the $2-x$ O-ions are statistically distributed.

Electroneutrality condition determines that site fractions on the two sublattices are not independent: Single variable y is equal $2-x$.

$$y_{\text{Ce}^{+3}} = y$$

$$y_{\text{Va}} = \frac{y}{4}$$

$$y_{\text{Ce}^{+4}} = (1-y)$$

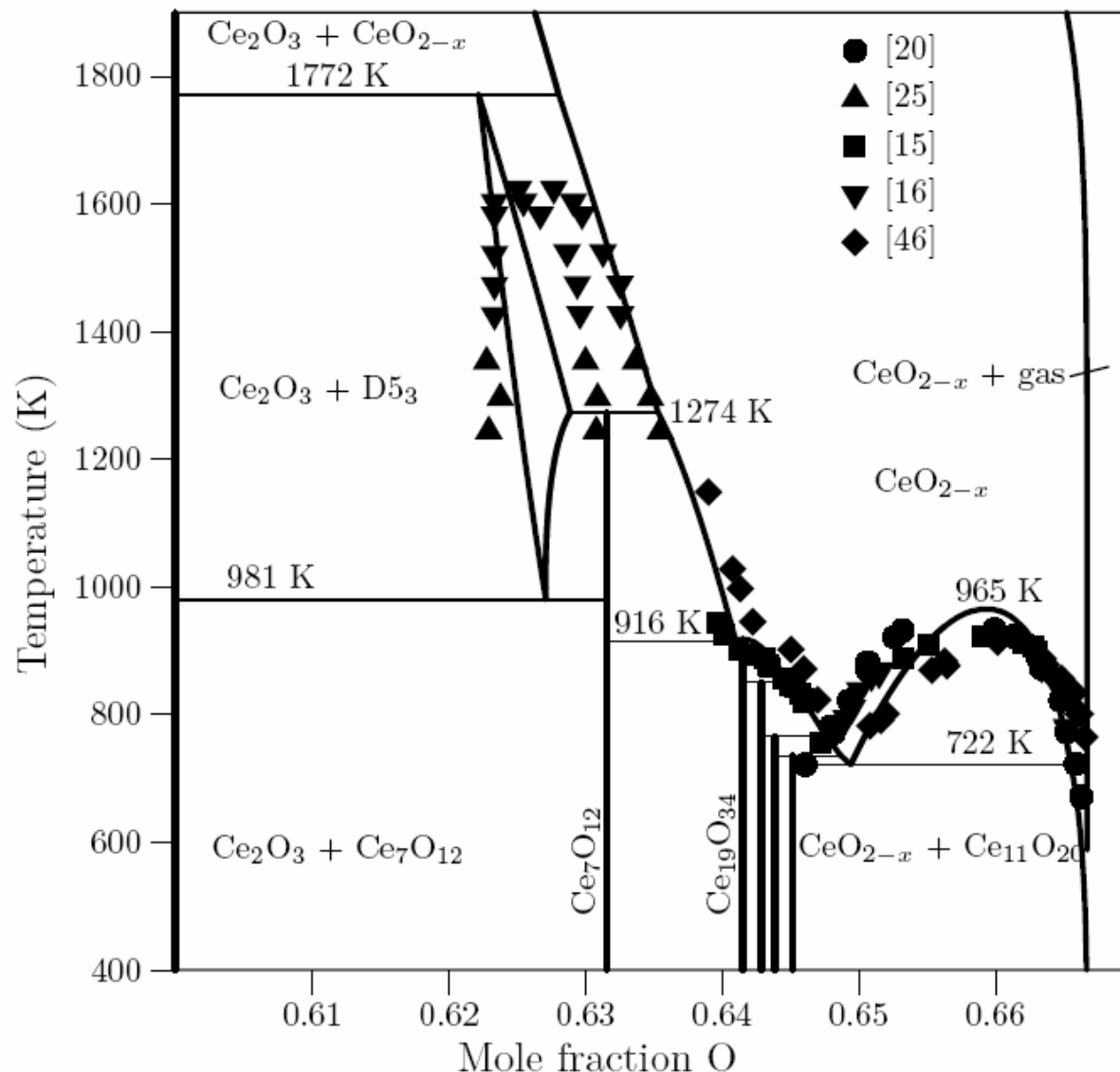
$$y_{\text{O}^{-2}} = \frac{1-y}{4}$$

No.	Paper	Experimental Technique	Measured Quantity	Composition	Temperature (K)	Remark
1.	Bevan & Kordis (1964)	Experiment with CO ₂ /CO & H ₂ O/H ₂	Partial pressures O ₂	CeO _{1.5-} CeO ₂	909 - 1442	+
2.	Ackerman & Rauh (1971)	Mass Spectroscopy & Mass Effusion	Partial pressures CeO, CeO ₂ , Ce(g), CeO	CeO _{1.51 -} CeO _{1.53} CeO _{1.5 -} CeO _{1.34}	2000 - 3000 1600 - 2000 1825 - 2320 1550 – 2040	+
3.	Iwasaki & Katsura (1971)	Experiment with CO ₂ & CO ₂ /H ₂ mixture	Partial pressures O ₂	CeO _{2.00}	900, 1000, 1100, 1227, 1300	+
4.	Campserveux & Gerdanian (1978)	Micro-Calorimetry	Partial pressures O ₂	CeO ₂	1353, 1296, 1244	+
5.	Kitayama et al. (1985)	Thermo-gravimetry	Partial pressures O ₂	CeO ₂ , Ce ₂ O ₃ Ce ₃ O ₅	1000 – 1330	+

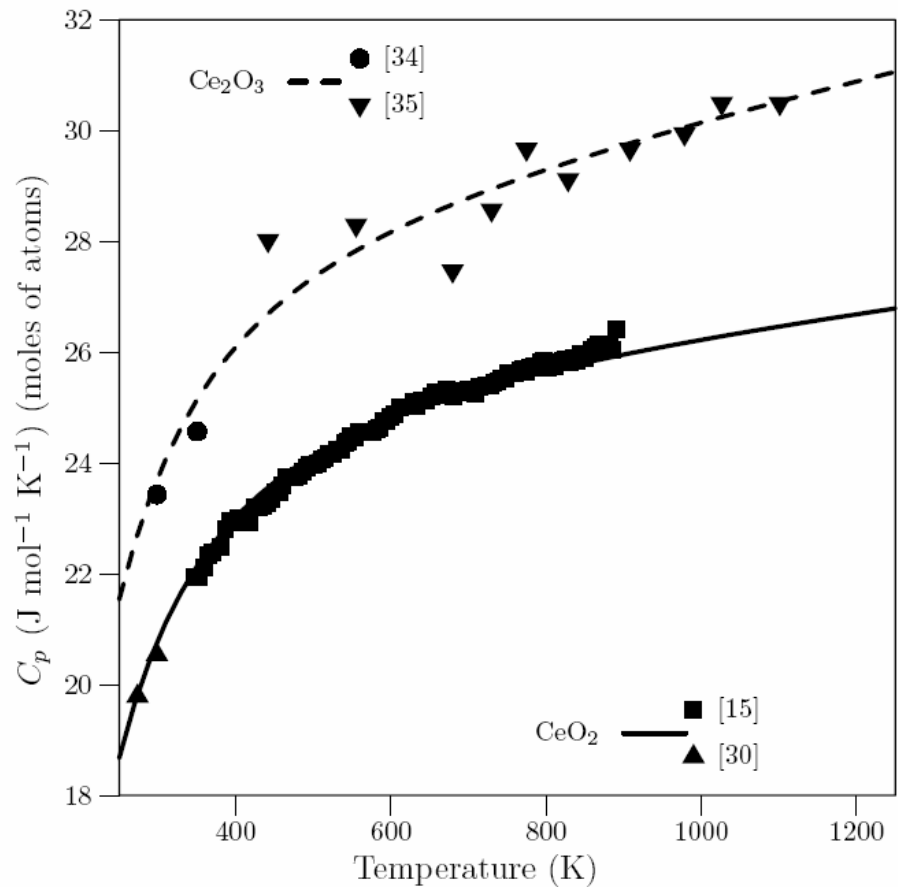
6.	Marushkin et al. (2000)	Knudsen cell, Mass spectrometry	Partial pressures, CeO_2 , Ce_2O_3	$\text{CeO}_{1.99}$, $\text{Ce}_2\text{O}_{2.96}$	1900-2150 1850-2050	-
7.	Kuznetzov& Rezukhina (1960)	Calorimetry	Heat capacity,	CeO_2	608-1172	-
8.	Westrum & Beale Jr. (1961)	Adiabatic Calorimetry	Heat capacity,	CeO_2	5-300	+
9.	Justice & Westrum (1969)	Cryogenic Calorimetry	Heat capacity	$\text{Ce}_2\text{O}_{3.02}$	5-350	+
10.	Basily & El-Sharkawy (1979)	Plane temperature wave method	Heat capacity	Ce_2O_3	400-1000	+
11.	Ricken et al. (1984)	Calorimetry	Specific heat, $\Delta H_{\text{trans.}}$	$\text{CeO}_{1.72} - \text{CeO}_2$	320-1200	-
12.	Kuznetzov, et al. (1960)	Bomb calorimetry	ΔH for Ce_2O_3	$\text{Ce}_2\text{O}_{3.00}$	298	+

13.	Baker & Holley (1968)	Oxygen Bomb Calorimetry	Heat of combustion Ce_2O_3	Ce_2O_3	298.15	-
14.	Baker, Huber, Holley & Krikorian (1971)	Bomb calorimetry	Heat of formation CeO_2 , $\text{CeC}_{1.5}$, CeC_2	CeO_2	298.15	-
15.	Campserveux & Gerdanian (1974)	Micro Calorimetry	Partial molal enthalpy $\Delta H_{\text{soln.}}(\text{O}_2)$	$\text{CeO}_{1.5} - \text{CeO}_2$	1353	+
16.	Panlener, Blementhal & Garnier(1975)	Thermo-gravimetry	$\Delta W/W$	CeO_{2-x}	1023-1773	+
17	Riess, Koerner & Noelting (1988)	Dilatometry	Thermal expansion coefficient	$\text{CeO}_{1.79} - \text{CeO}_2$	320-1200	+

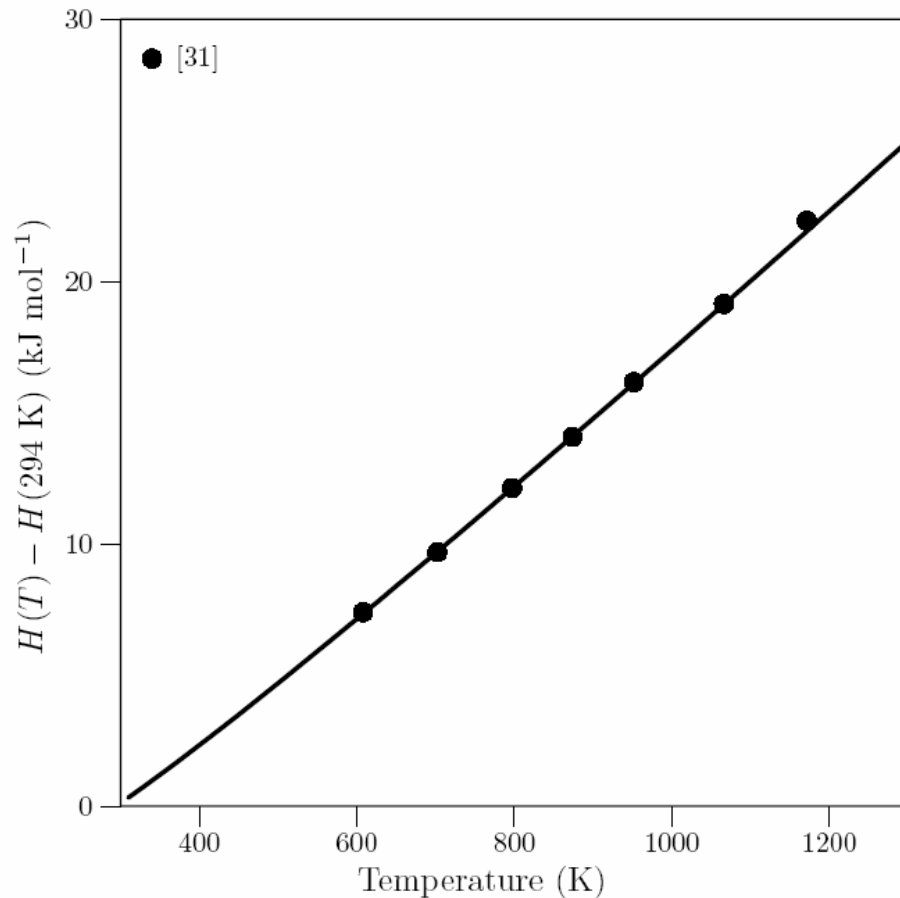
Calculated Ce–O System in Solid State from 60 to 67 mol. % O in comparison with experimental data.



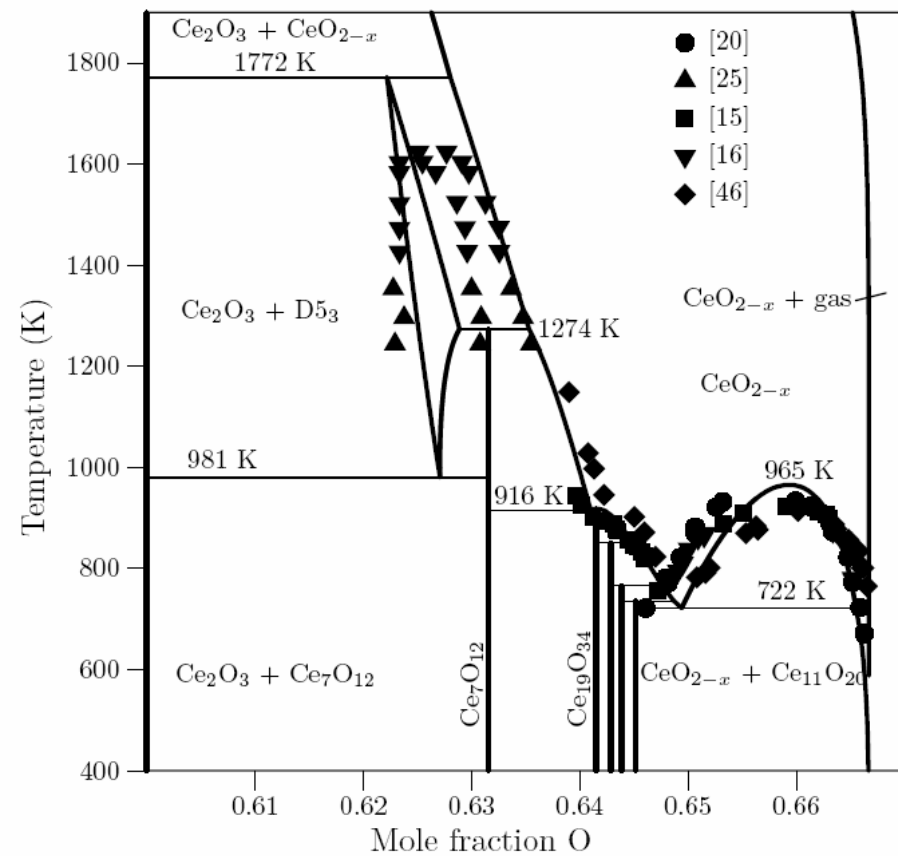
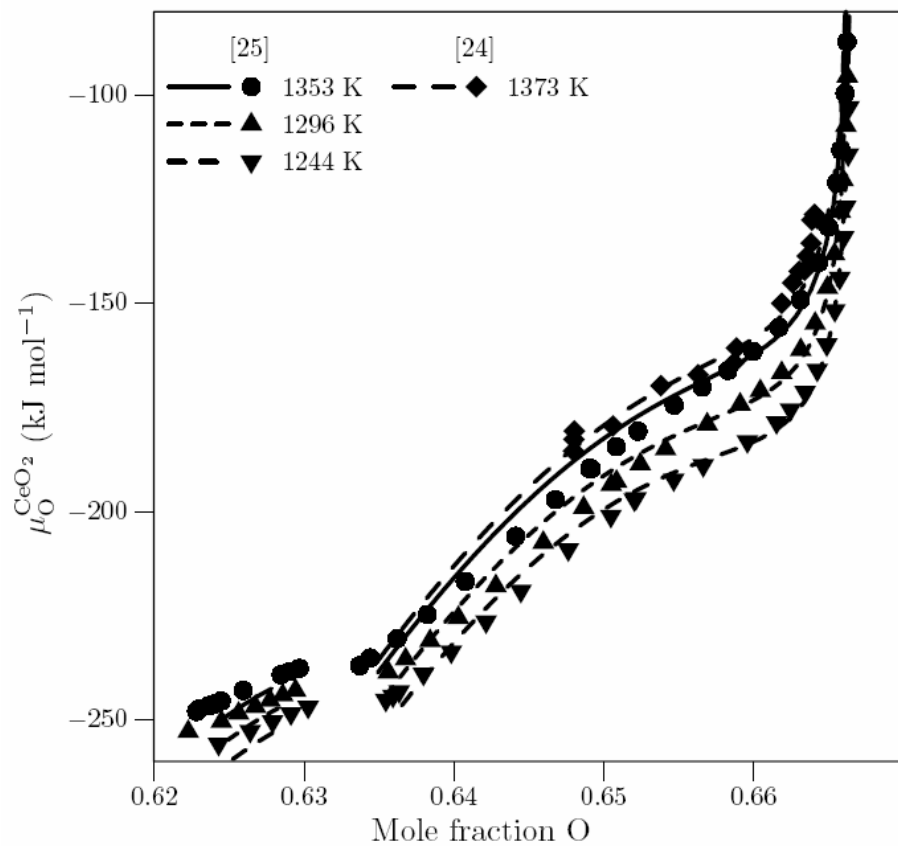
Heat capacities of Ce_2O_3 and CeO_2 .



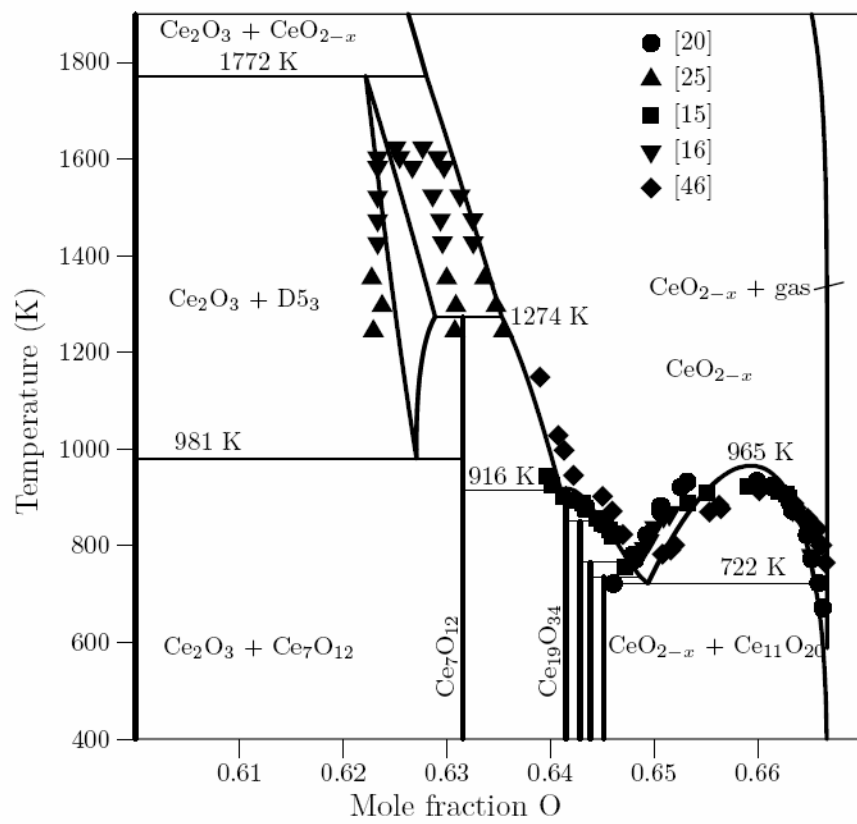
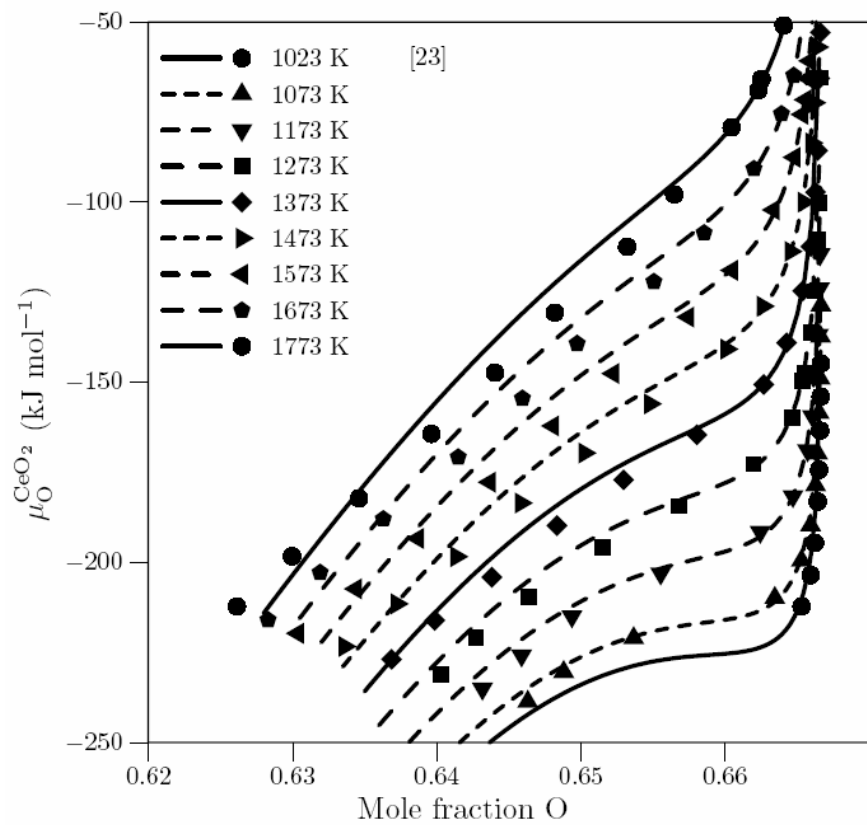
Enthalpy increment (heat contents) of CeO_2 .



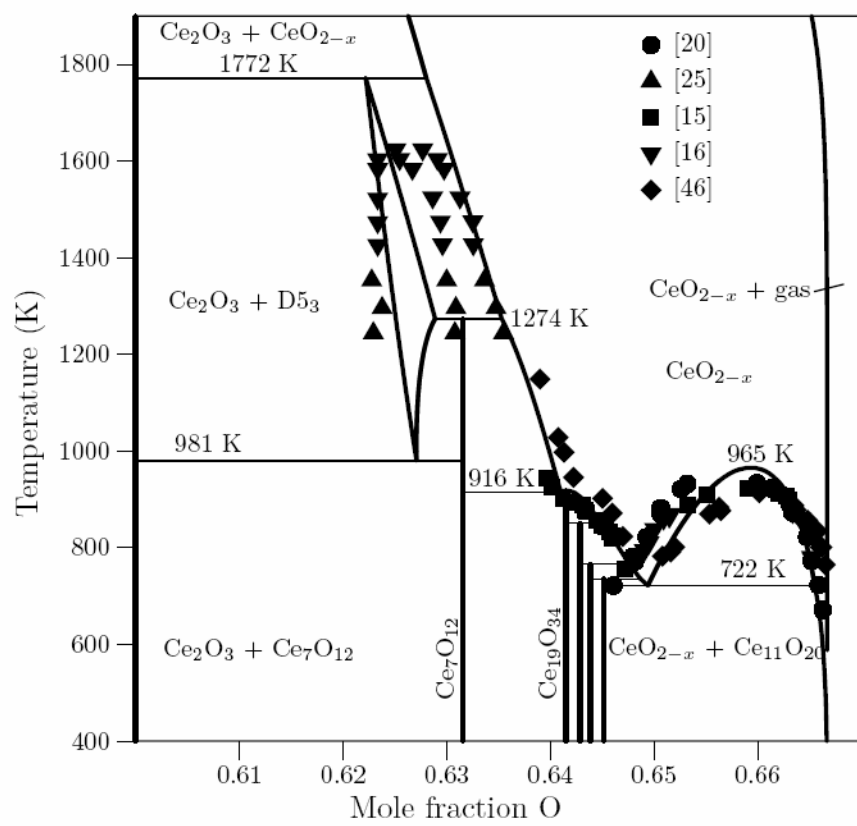
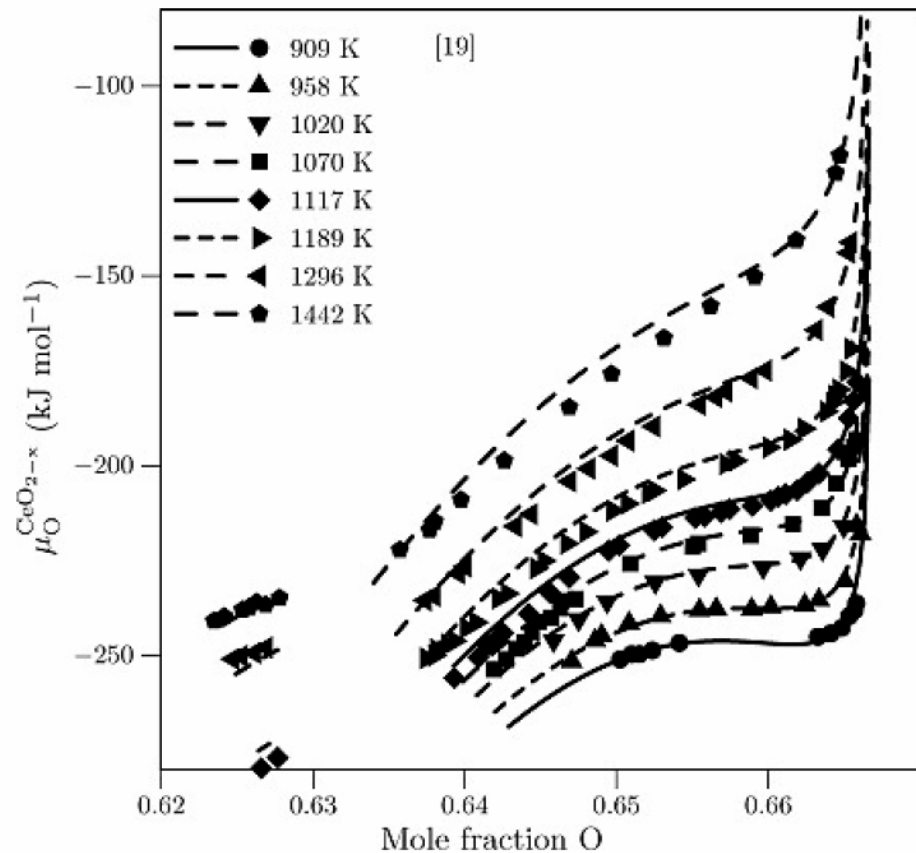
Chemical potentials of oxygen for ceria as a function of composition and temperature.



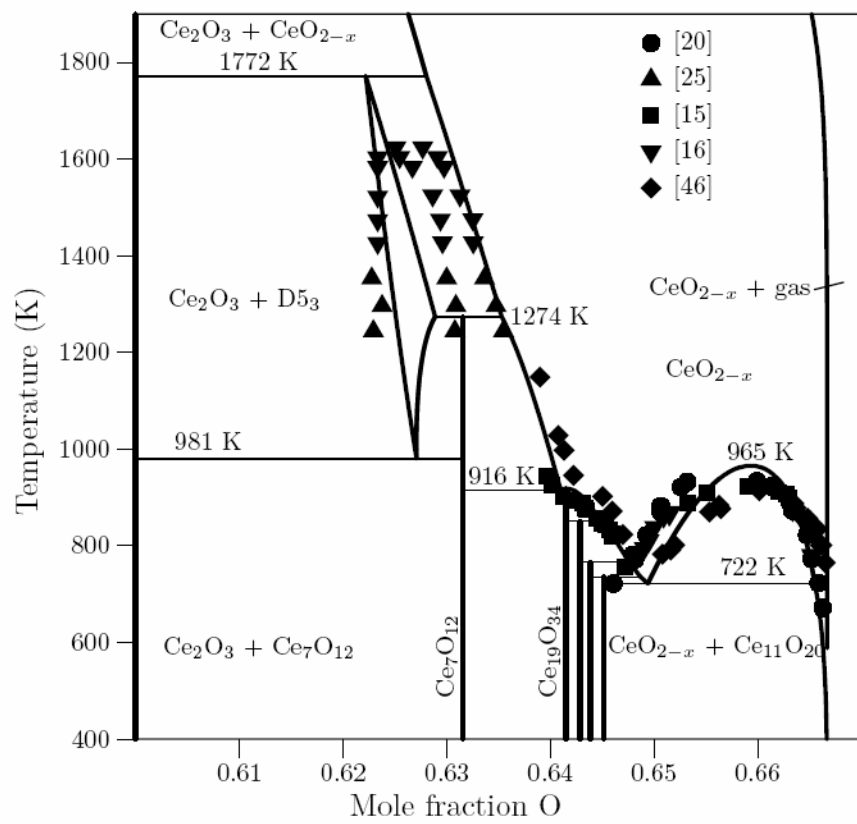
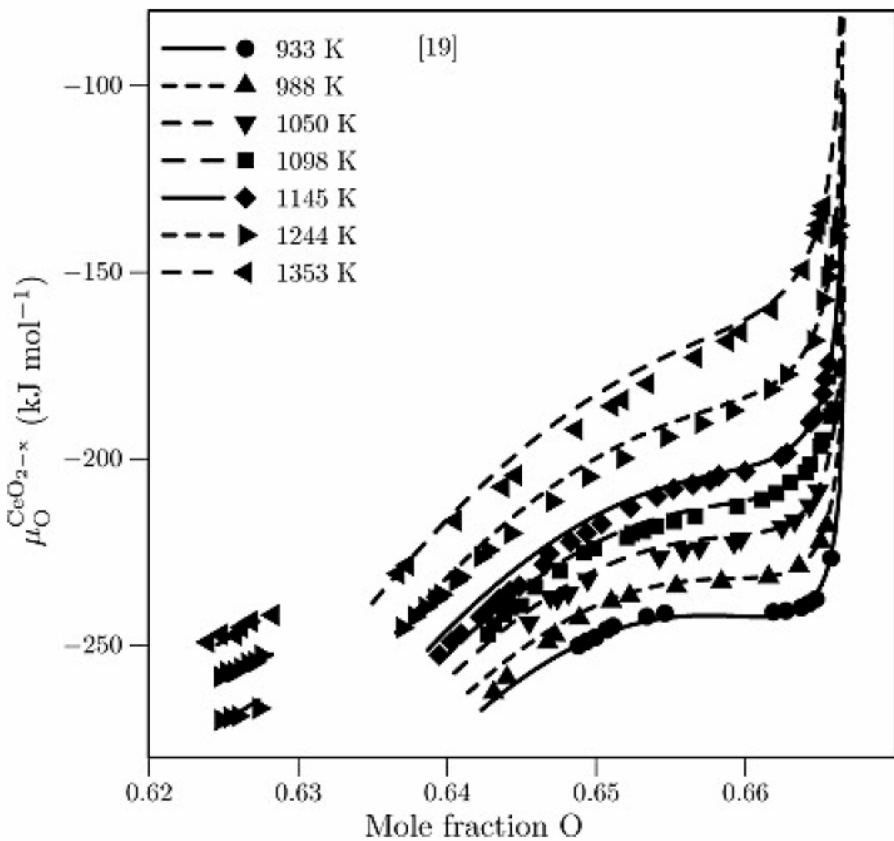
Chemical potentials of oxygen for ceria as a function of composition and temperature.



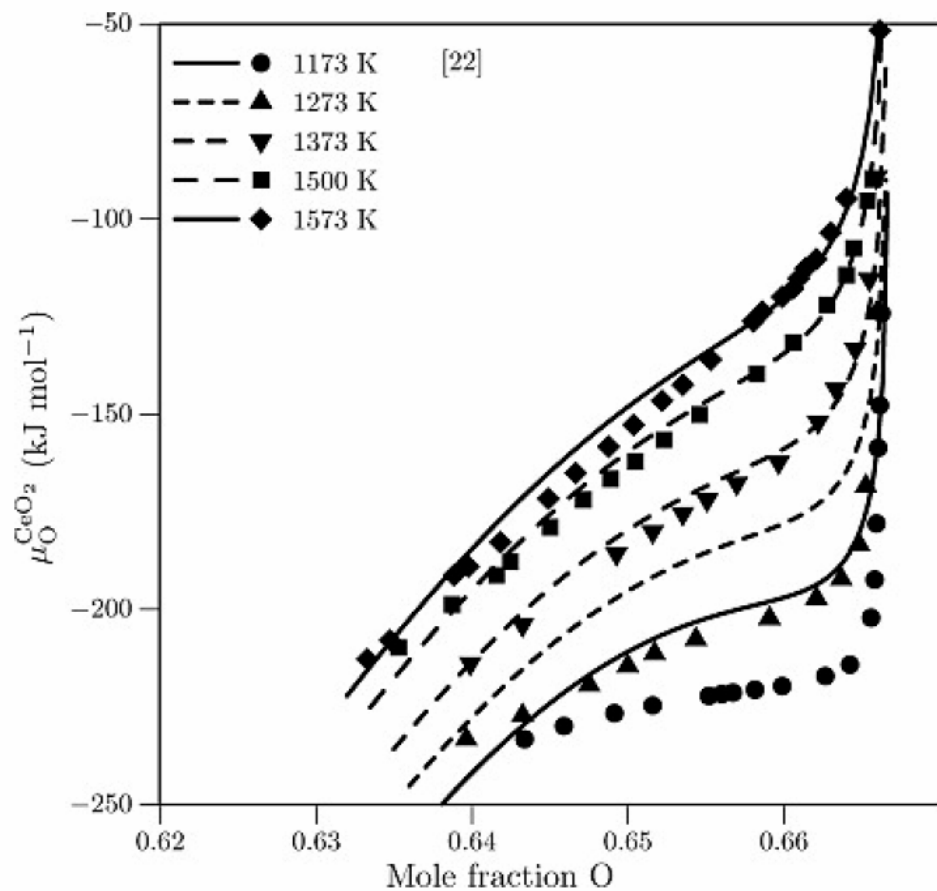
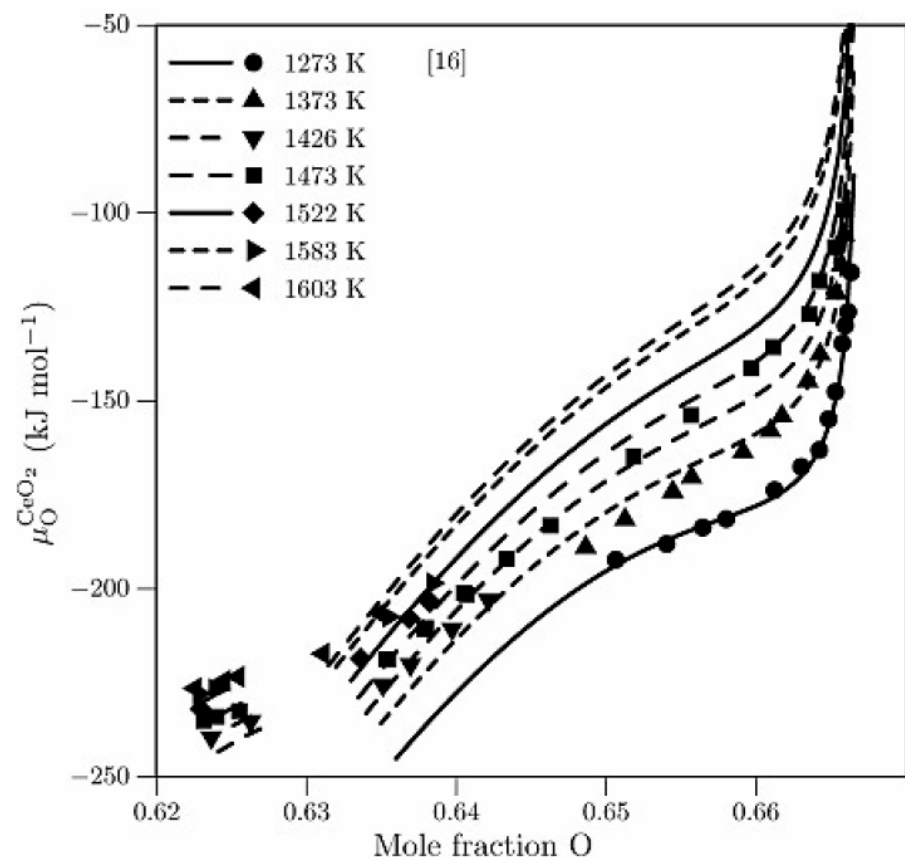
Chemical potentials of oxygen for ceria as a function of composition and temperature.



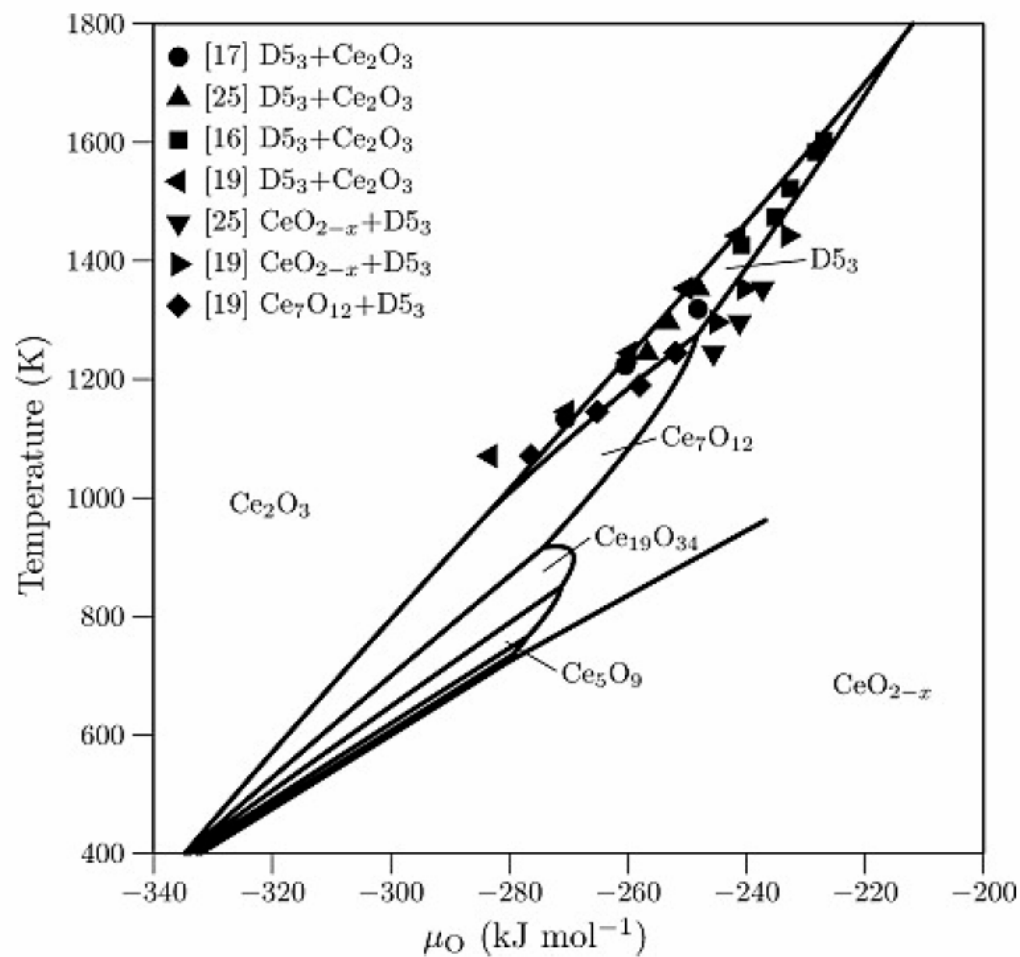
Chemical potentials of oxygen for ceria as a function of composition and temperature.



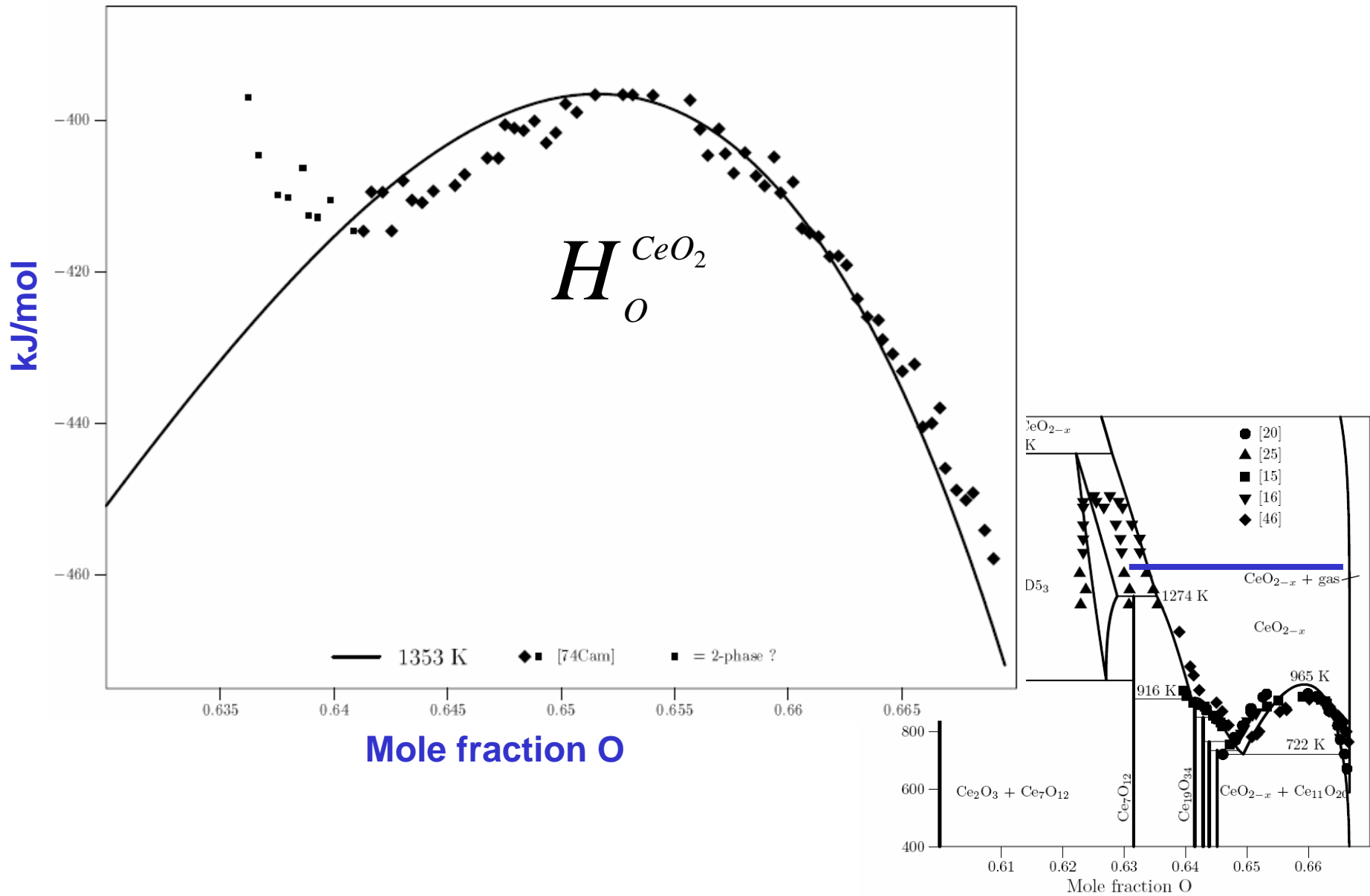
Chemical potentials of oxygen for ceria as a function of composition and temperature.



Chemical potentials of oxygen in the two-phase areas.



Partial Enthalpies of Oxygen in CeO_2



Thermodynamics of High Temperature Materials Systems

Hans Jürgen Seifert

Outline

1. Introduction and motivation for thermodynamic calculations

- Computational thermodynamics
- CALPHAD approach (CALculation of PHAse Diagrams)
- Thermodynamic databases and software

2. Thermodynamic optimization of the Ce-O system

- Thermodynamic modeling of solution phases

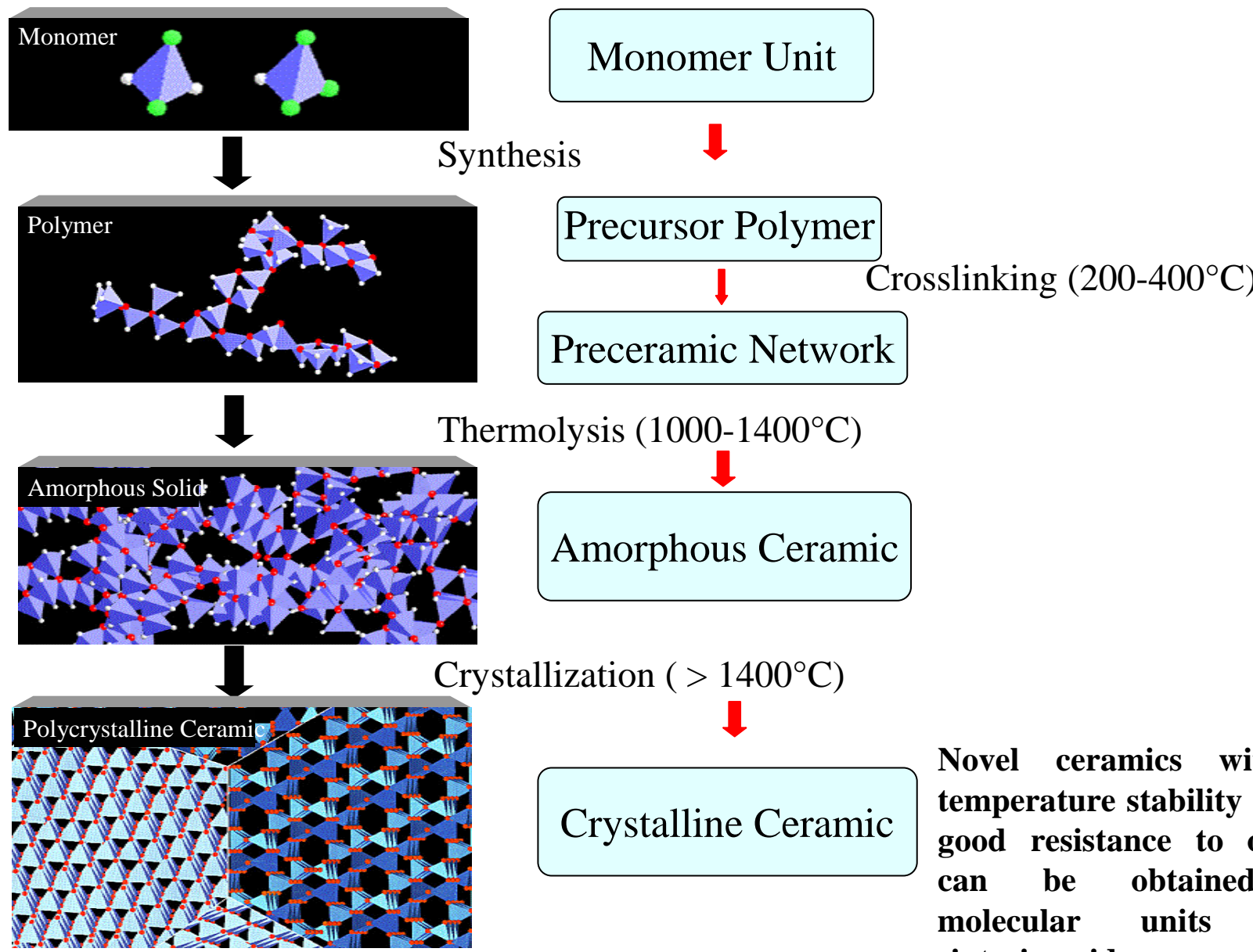
3. Precursor-derived Si-(B-)C-N ceramics

- High temperature reactions of silicon carbide and silicon nitride ceramics
 - Crystallization and high temperature stability of Si-(B-)C-N ceramics
-

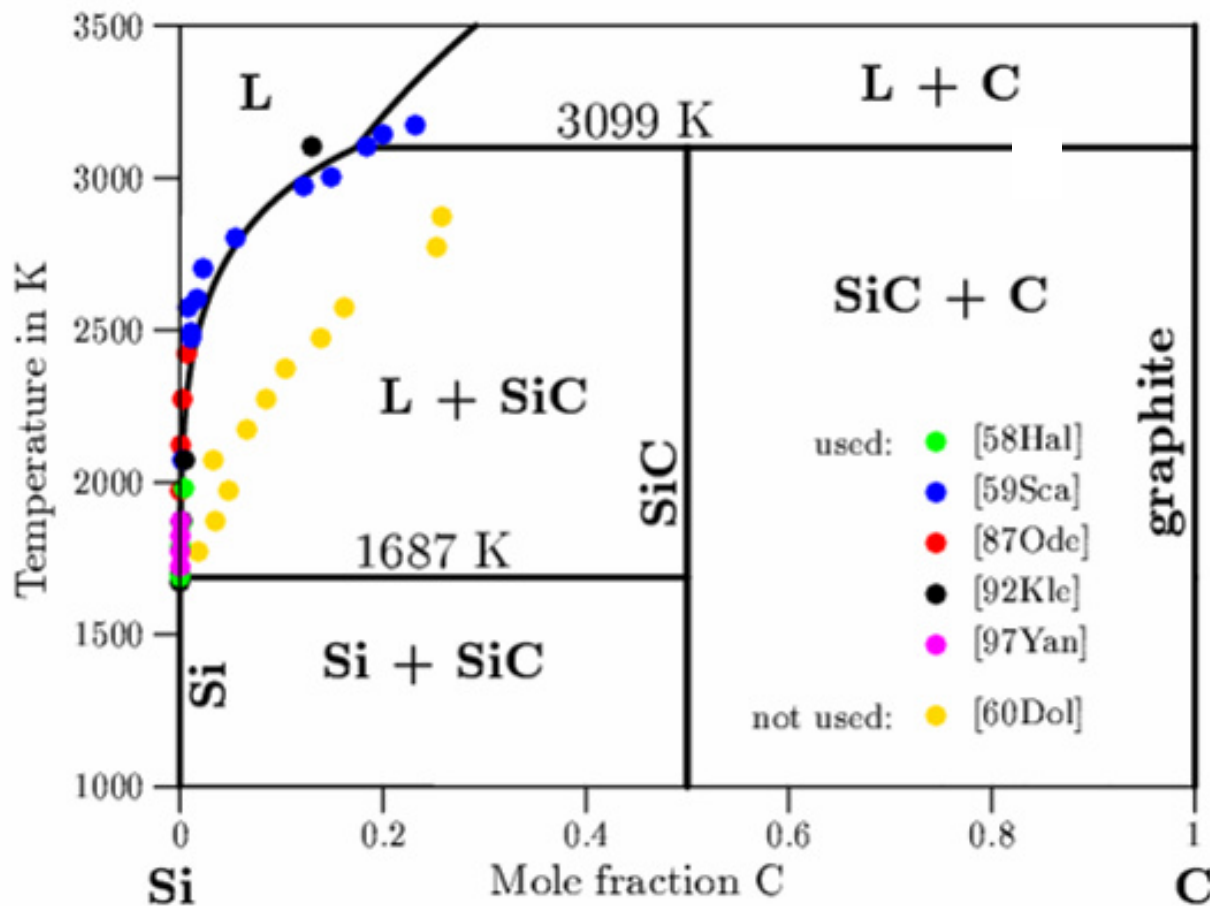
Precursor-derived Si-B-C-N Ceramics

- Produced by thermolysis (1323 K, Ar) of polymer precursors
- Amorphous, purely homogeneous inorganic materials
- NCP200: **40.1Si 23C 36.9N** (at.%)
 - Starts to crystallize at 1700 K (N_2)
 - Thermal stability up to 1800 K (N_2)
- T2-1: **29.1Si 41.7C 19.4N 9.8B** (at.%)
 - X-ray amorphous, nanocrystalline
 - Thermal stability up to 2300 K

Process for Precursor-derived Si-(B-)C-N Ceramics

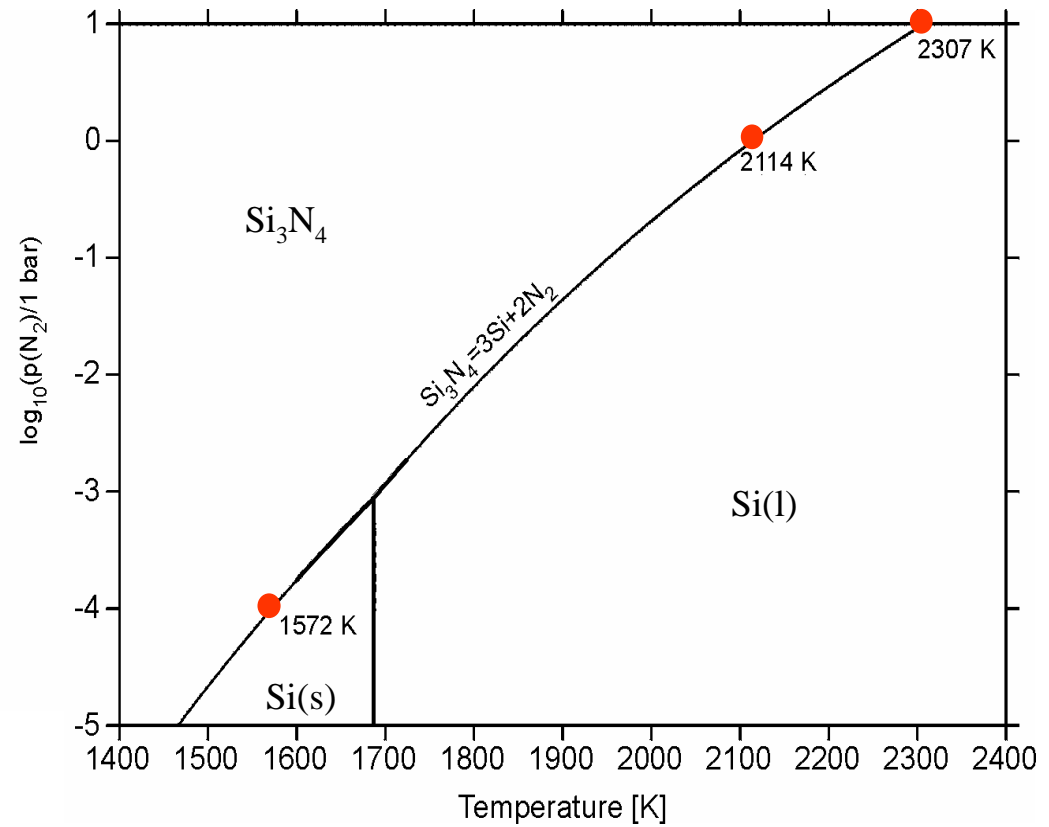
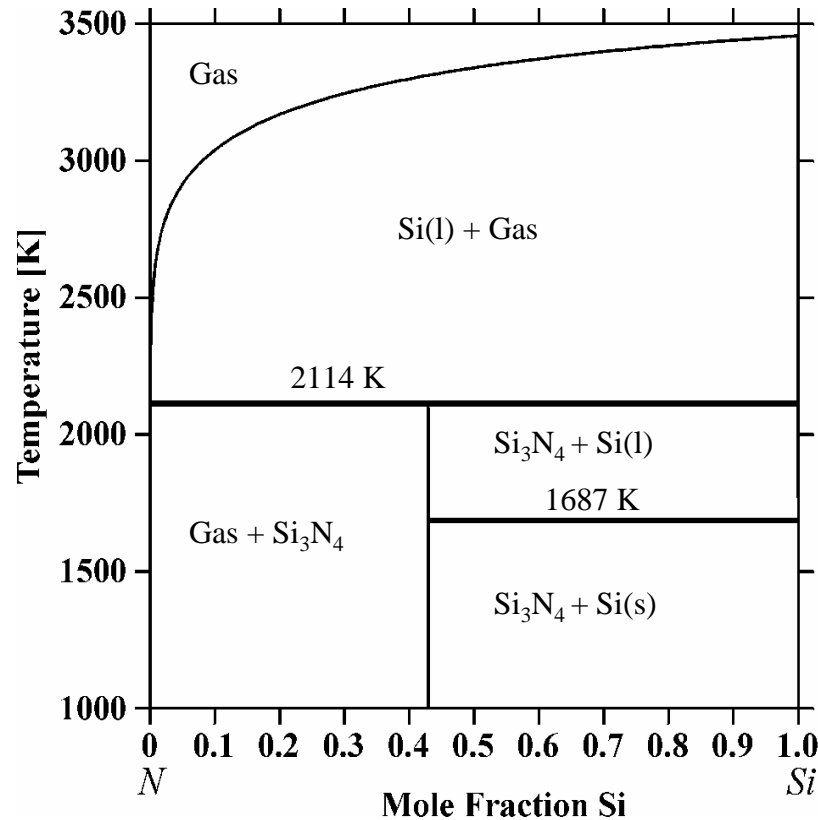


Si-C binary subsystem

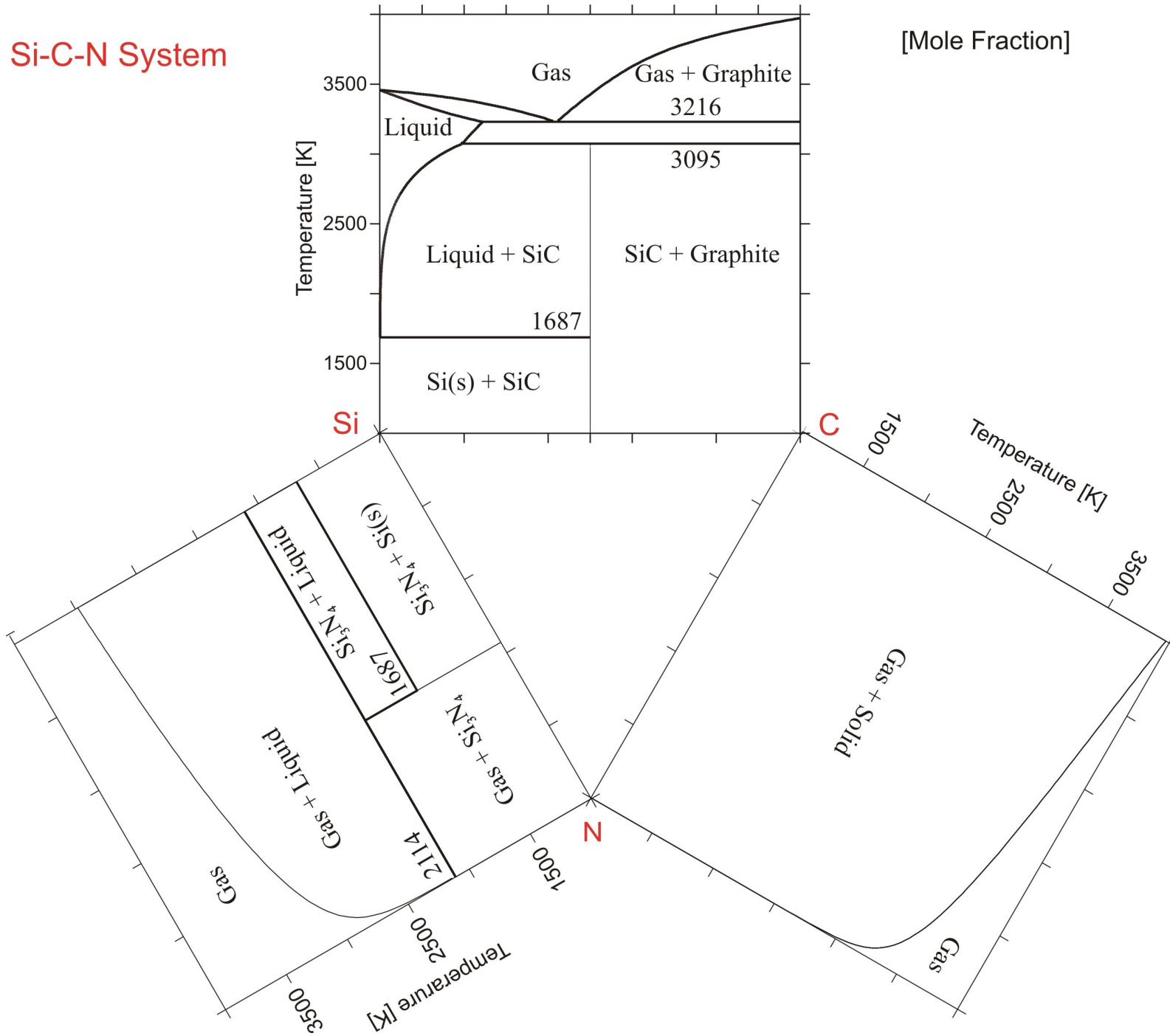


J. Gröbner, PhD thesis, 1994

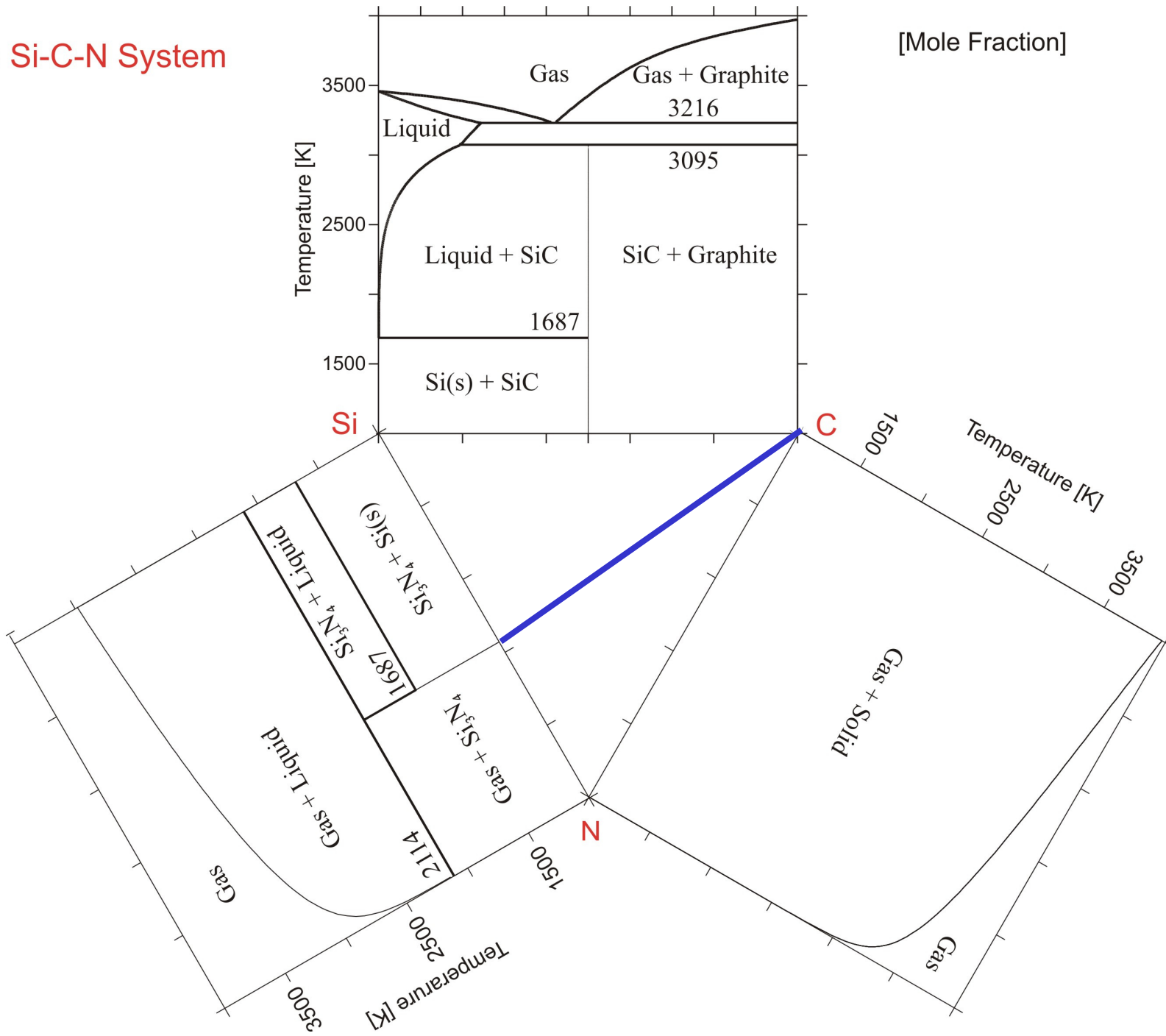
Si-N binary subsystem



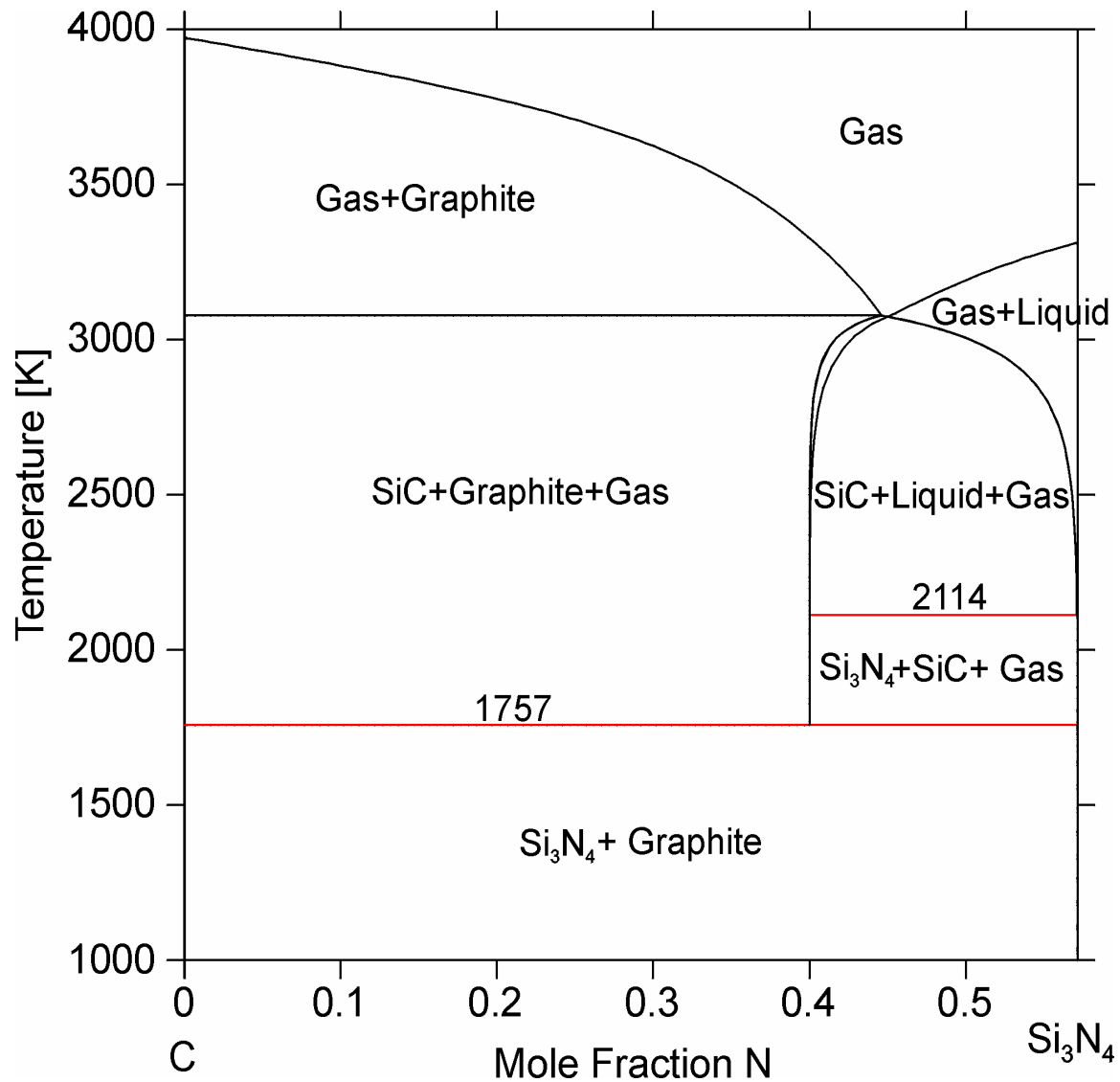
The Si-C-N System



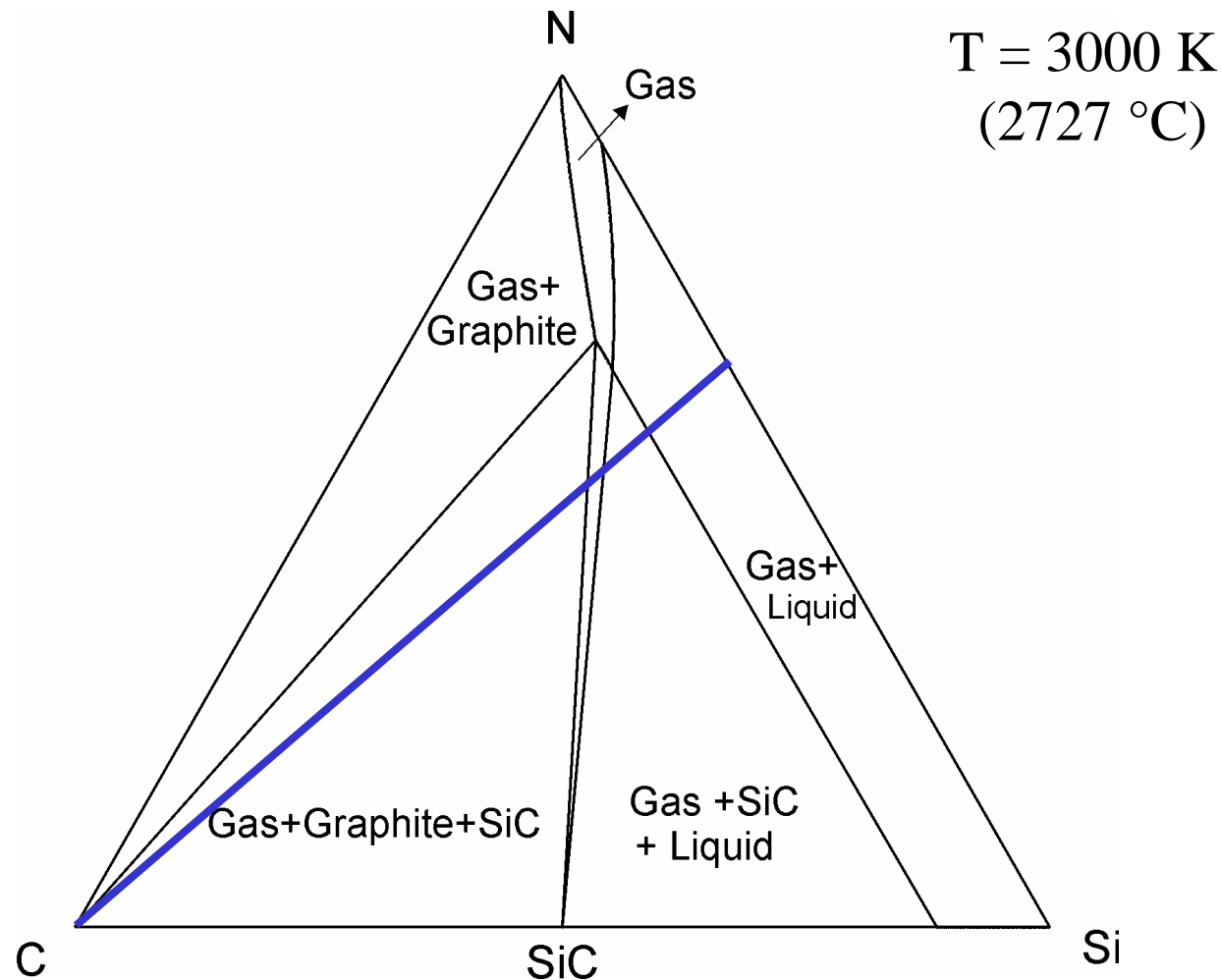
The Si-C-N System



Isopleth from Carbon to Si_3N_4 in the Si-C-N System

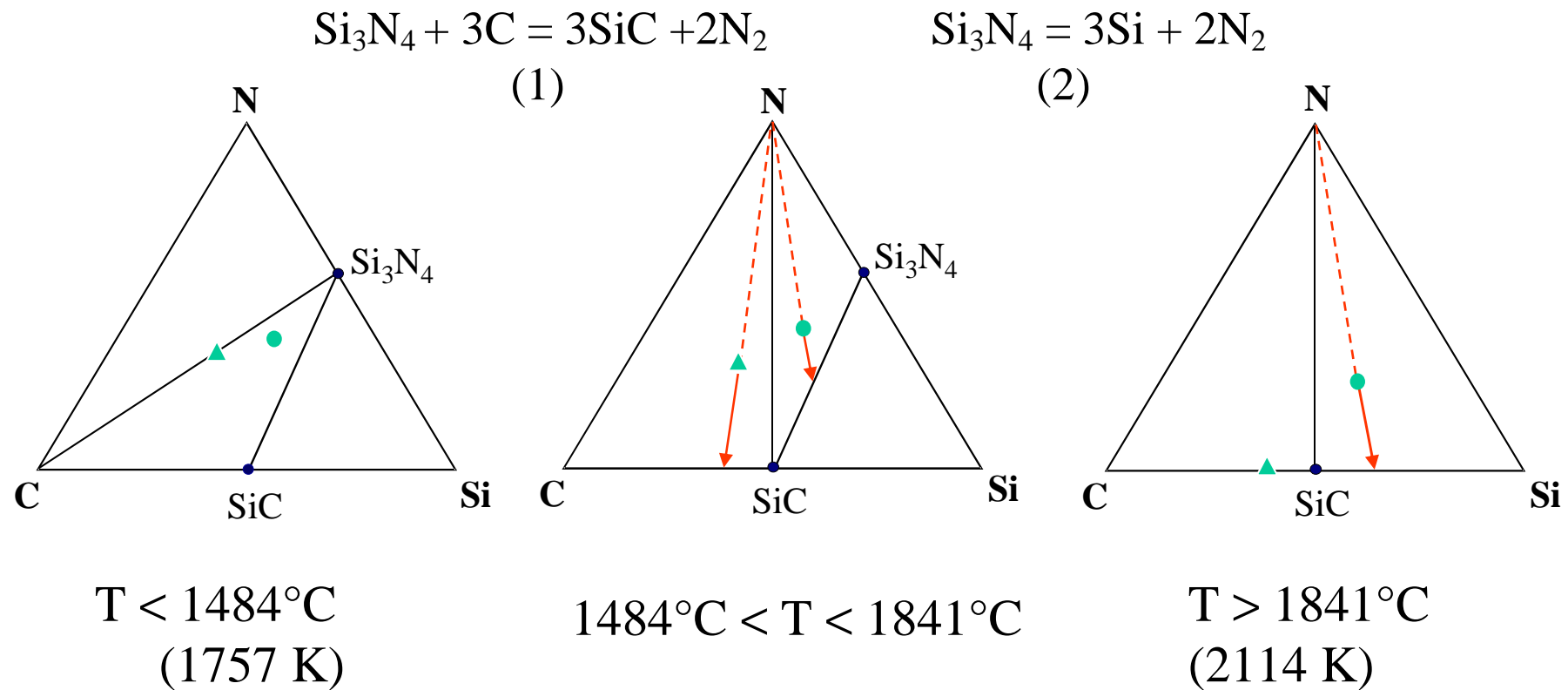


Isothermal Section of the Ternary System Si-C-N



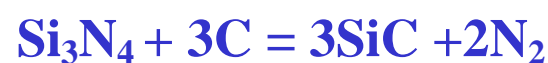
Isothermal Sections of the Ternary System Si-C-N

- ▲ $\text{Si}_1\text{N}_{1.6}\text{C}_{1.33}$ (**VT50**, Polyvinylsilazane, Hoechst AG, Frankfurt, Germany)
- $\text{Si}_1\text{N}_{0.6}\text{C}_{1.02}$ (**NCP200**, Polyhydridomethylsilazane, Nichimen Corp., Tokyo, Japan)

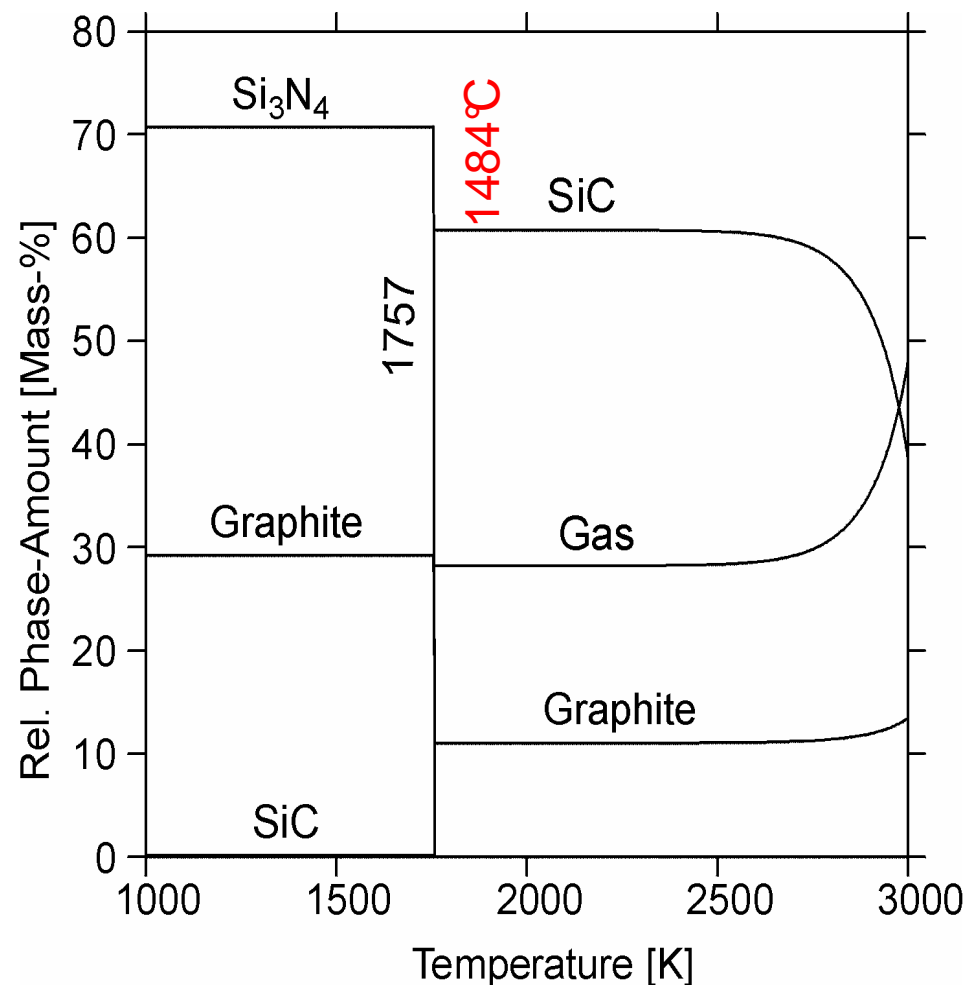


P = 1 bar

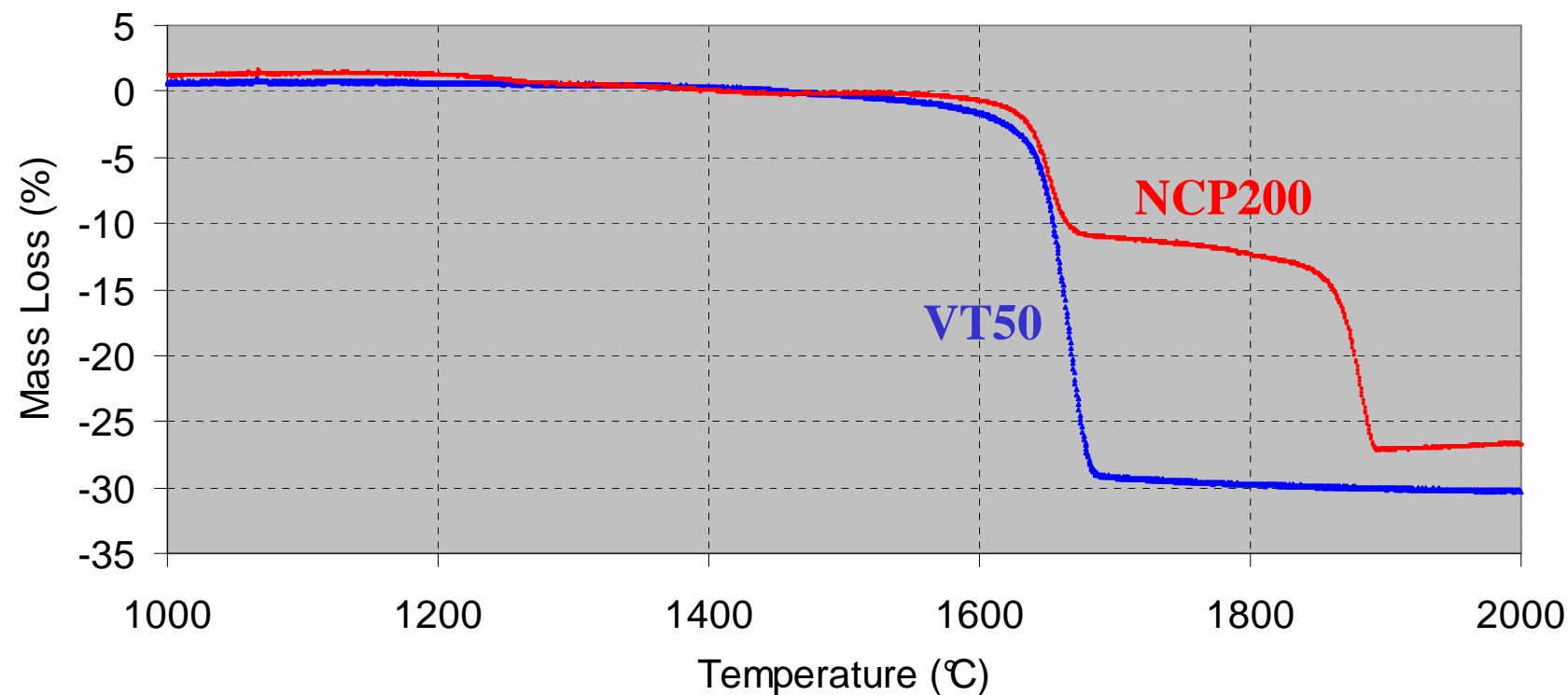
Calculated Phase Fraction Diagrams of Precursor Derived Ceramics



$\text{Si}_1\text{N}_{1.6}\text{C}_{1.33}$
(VT50)



Thermogravimetical (TG) analysis of precursor-derived Si-C-N ceramics



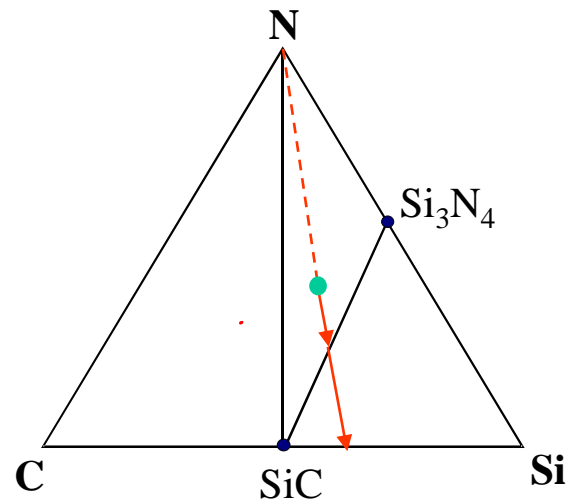
Calculated Phase Fraction Diagram of Precursor Derived Ceramics

NCP200, Polyhydridomethylsilazane (Nichimen Corp., Tokyo, Japan)

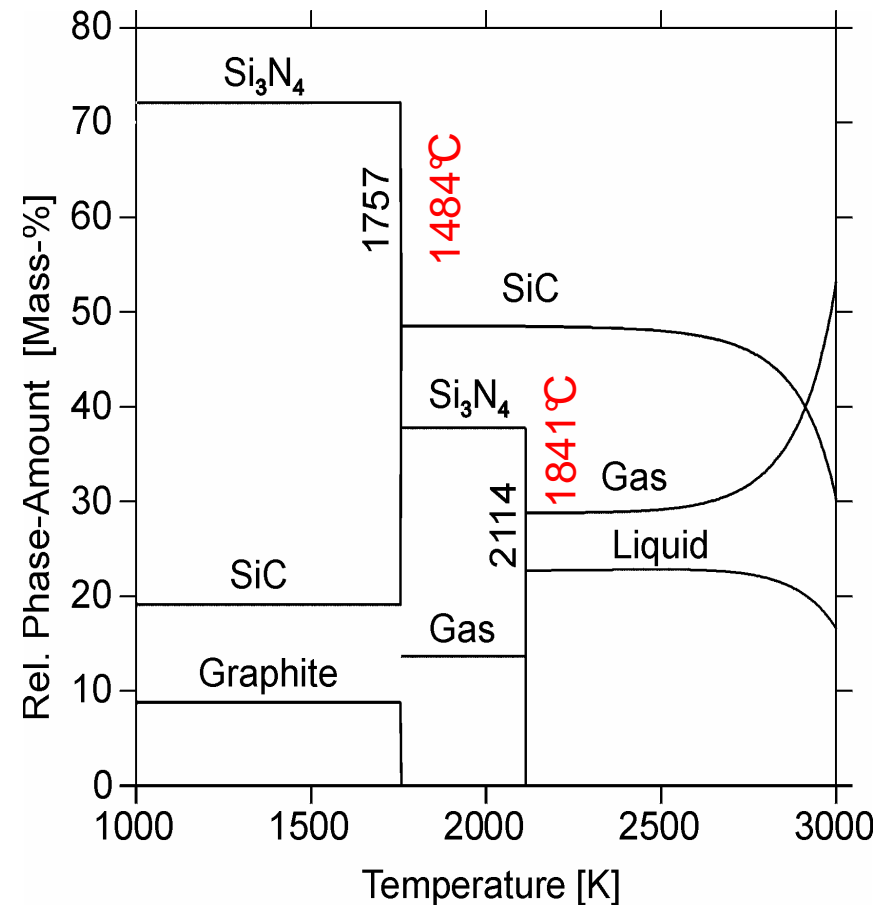
Ceramics:

$\text{Si}_1\text{N}_{0.6}\text{C}_{1.02}$

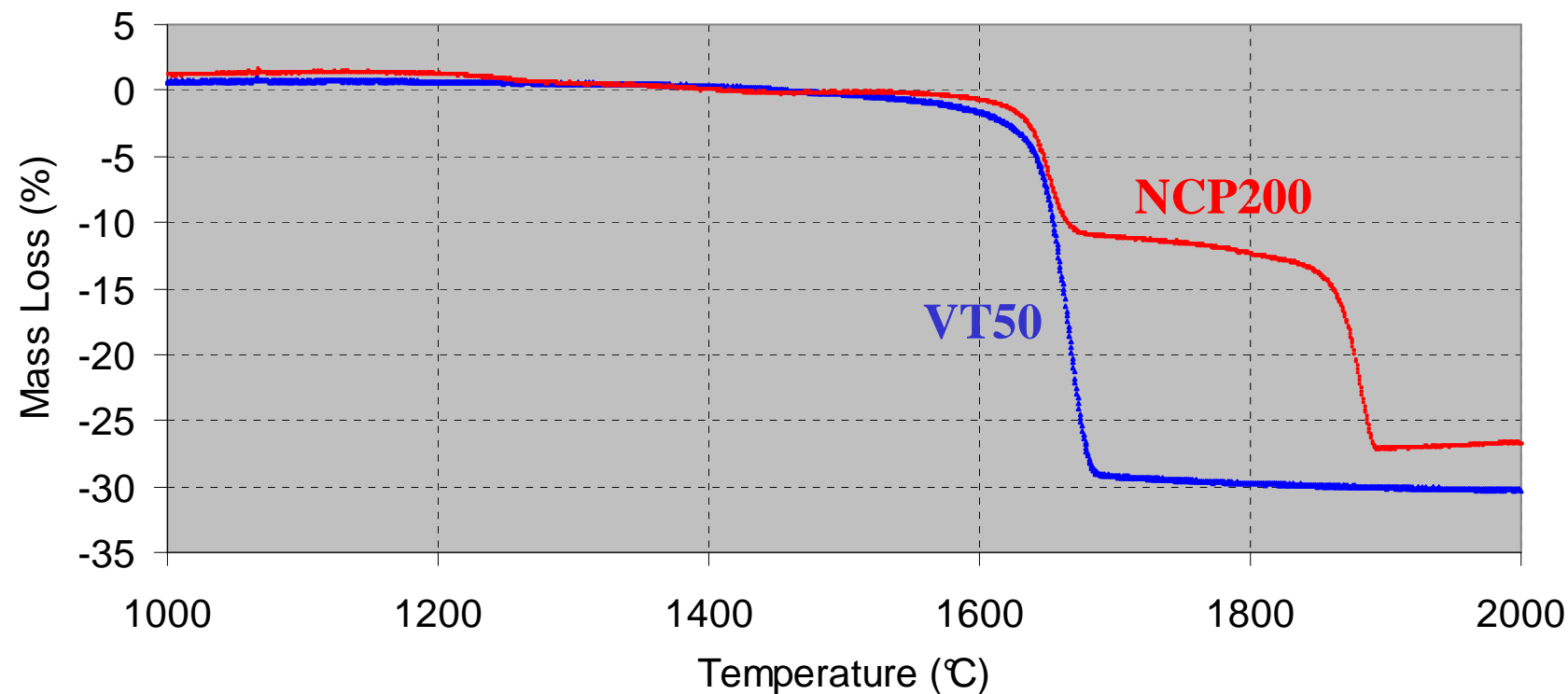
Reaction Path



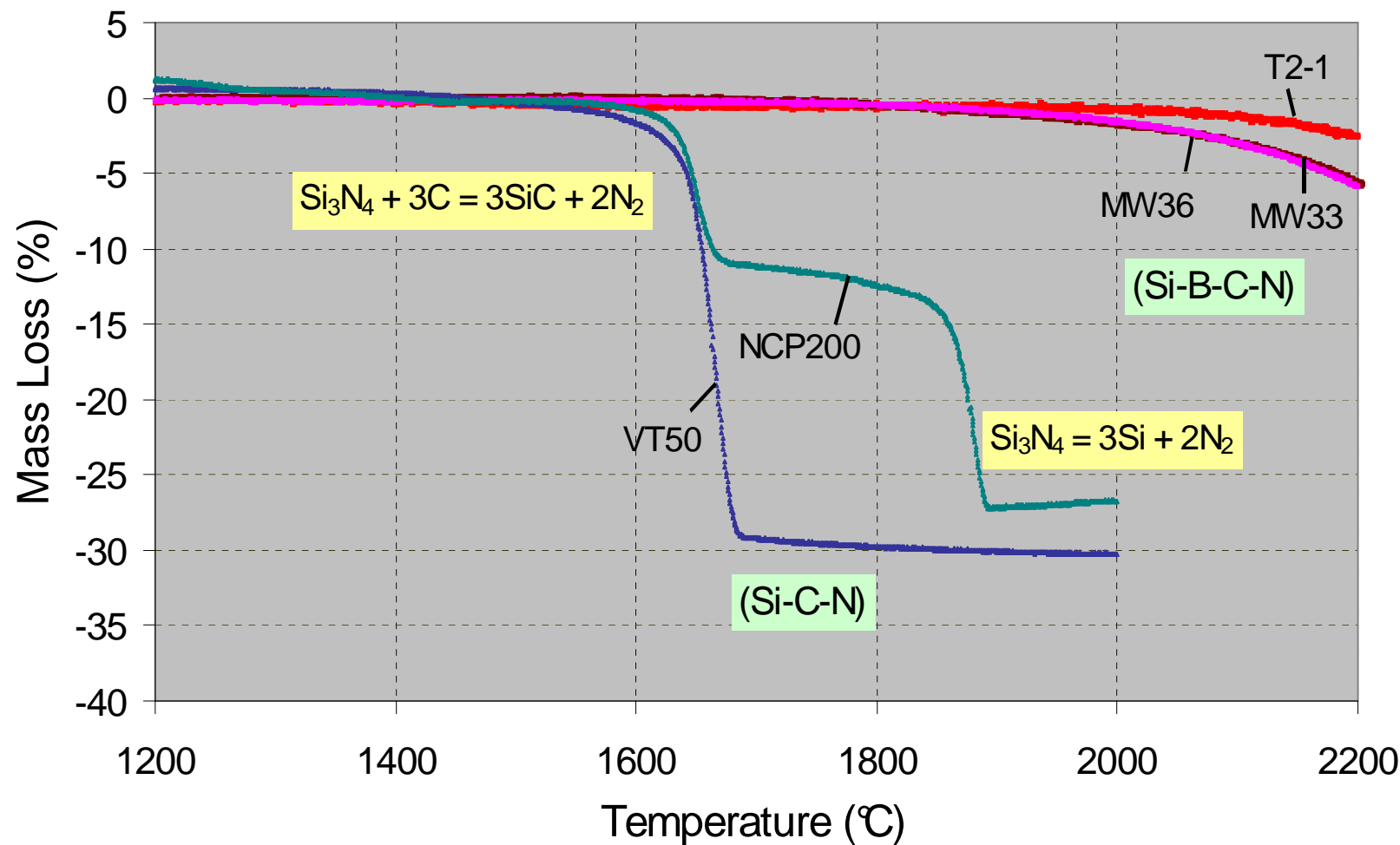
Phase Fraction Diagram



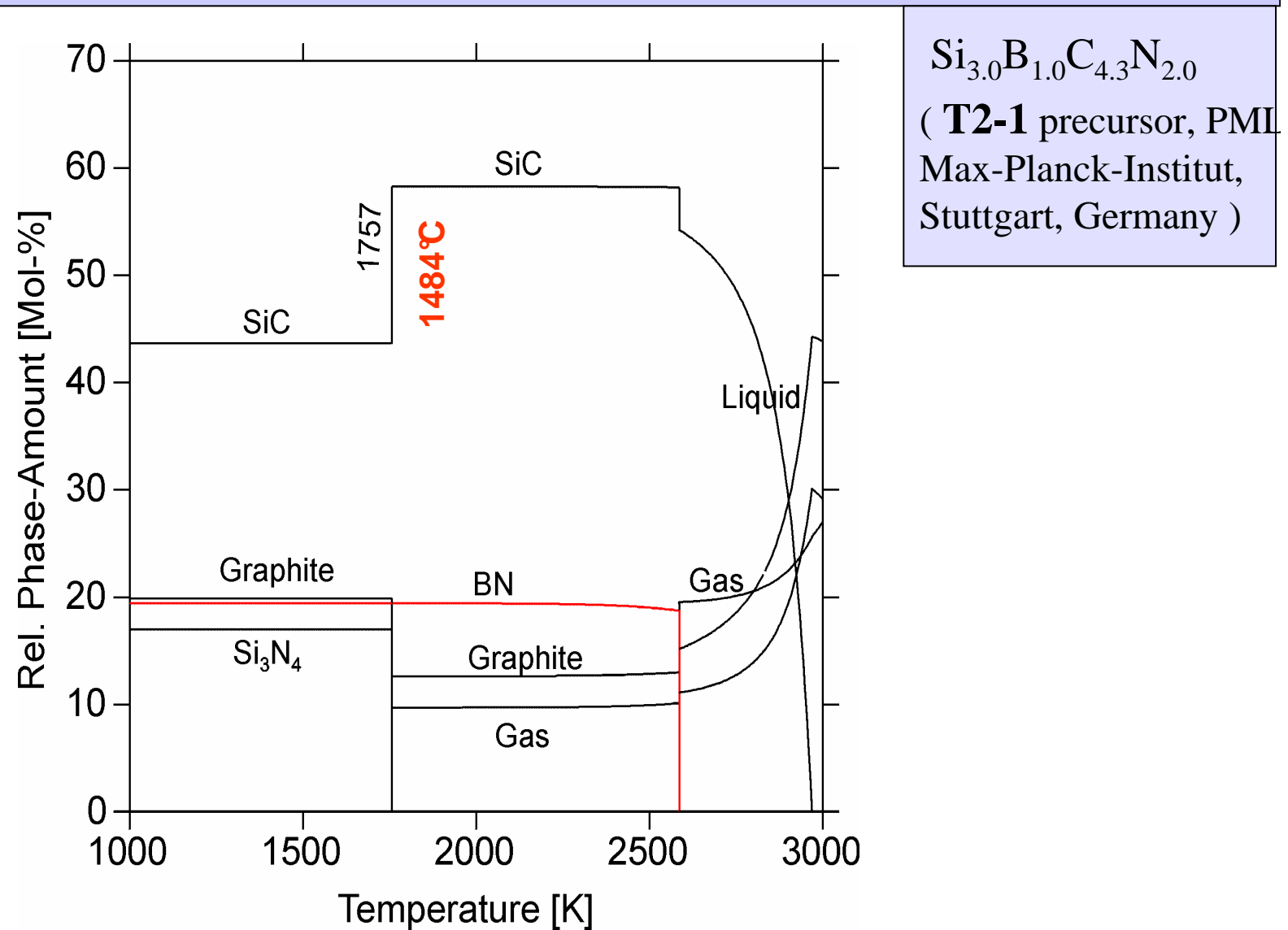
Thermogravimetical (TG) analysis of precursor-derived Si-C-N ceramics

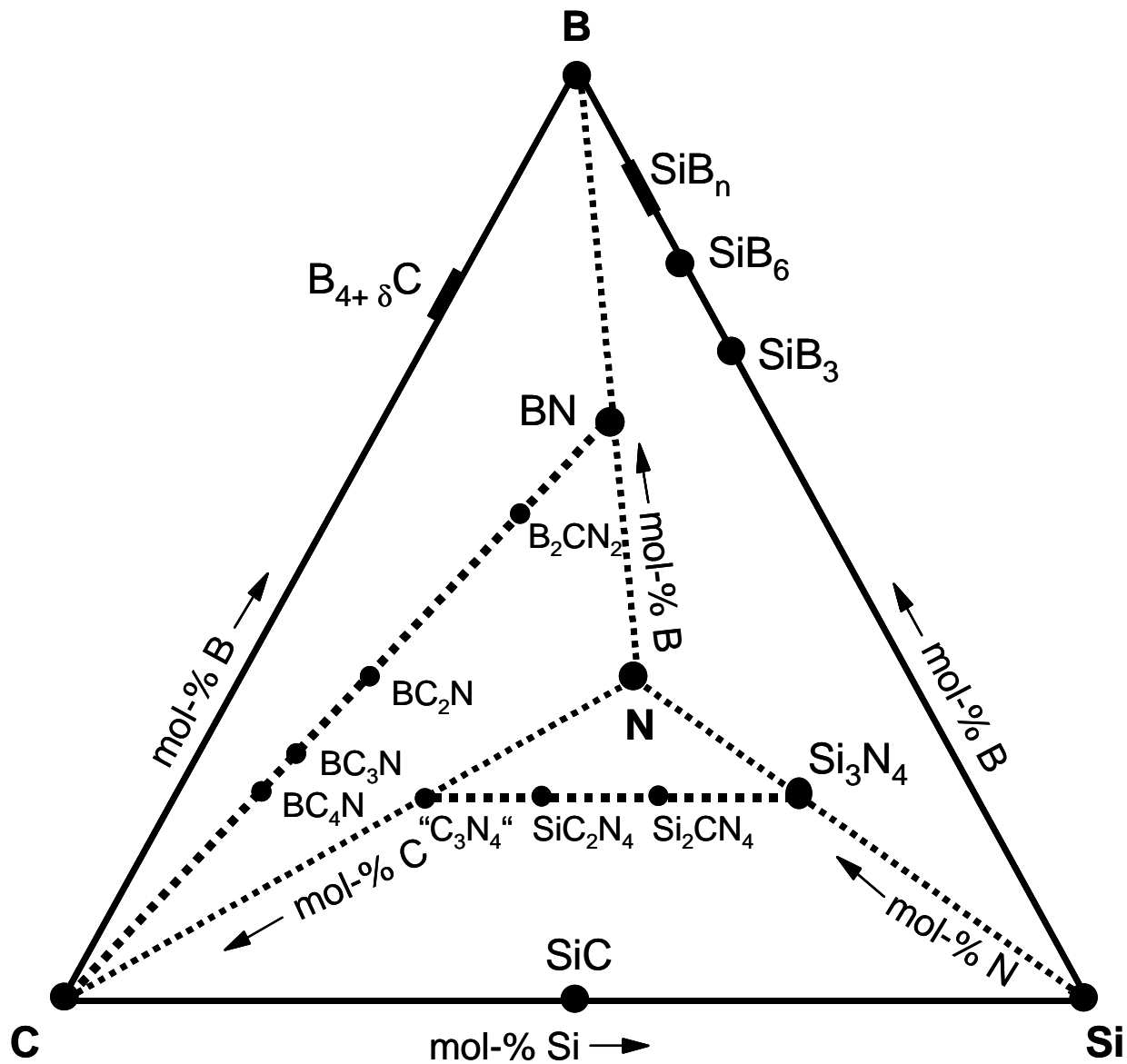


Thermogravimetical (TG) analysis of precursor-derived Si-B-C-N ceramics

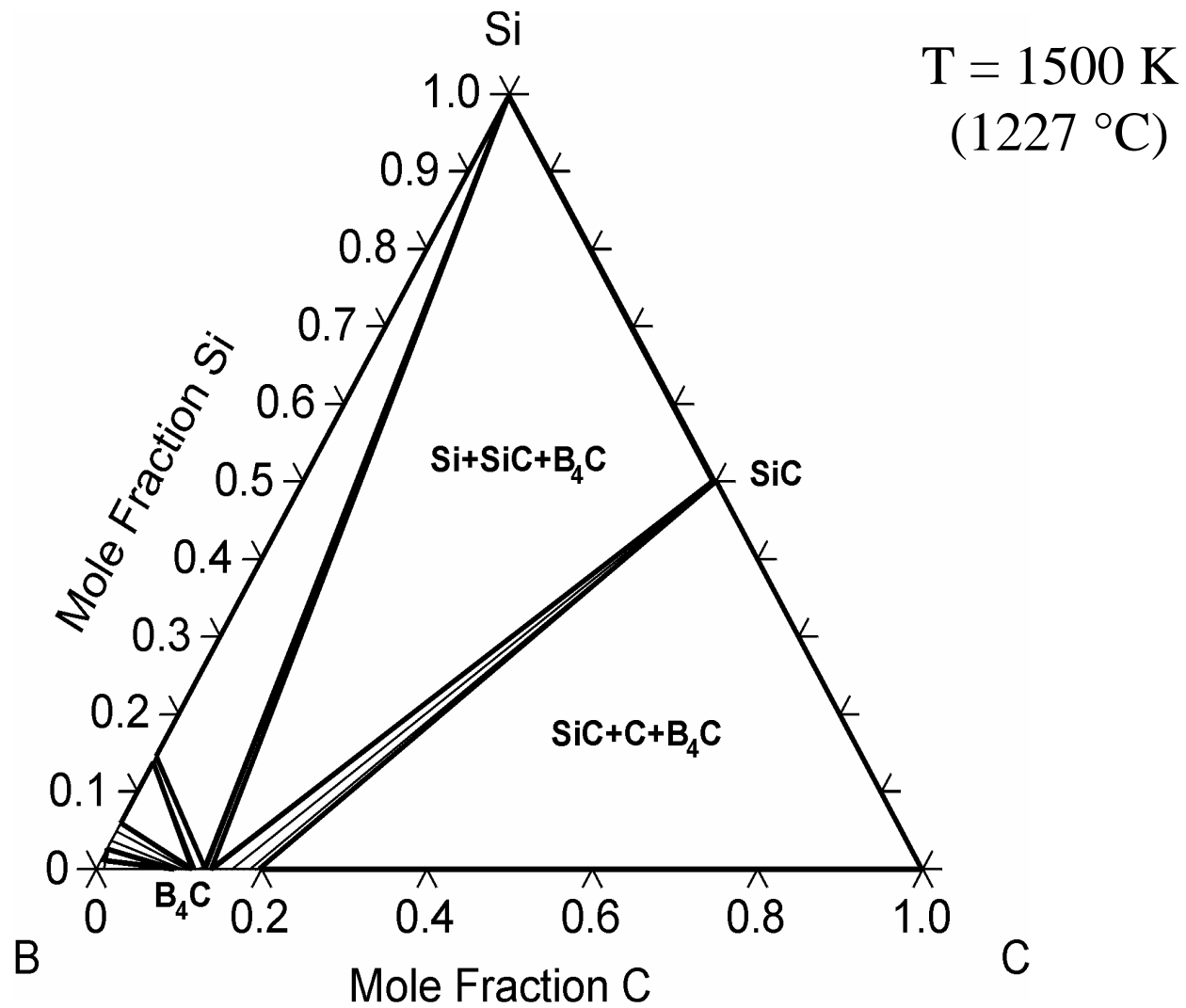


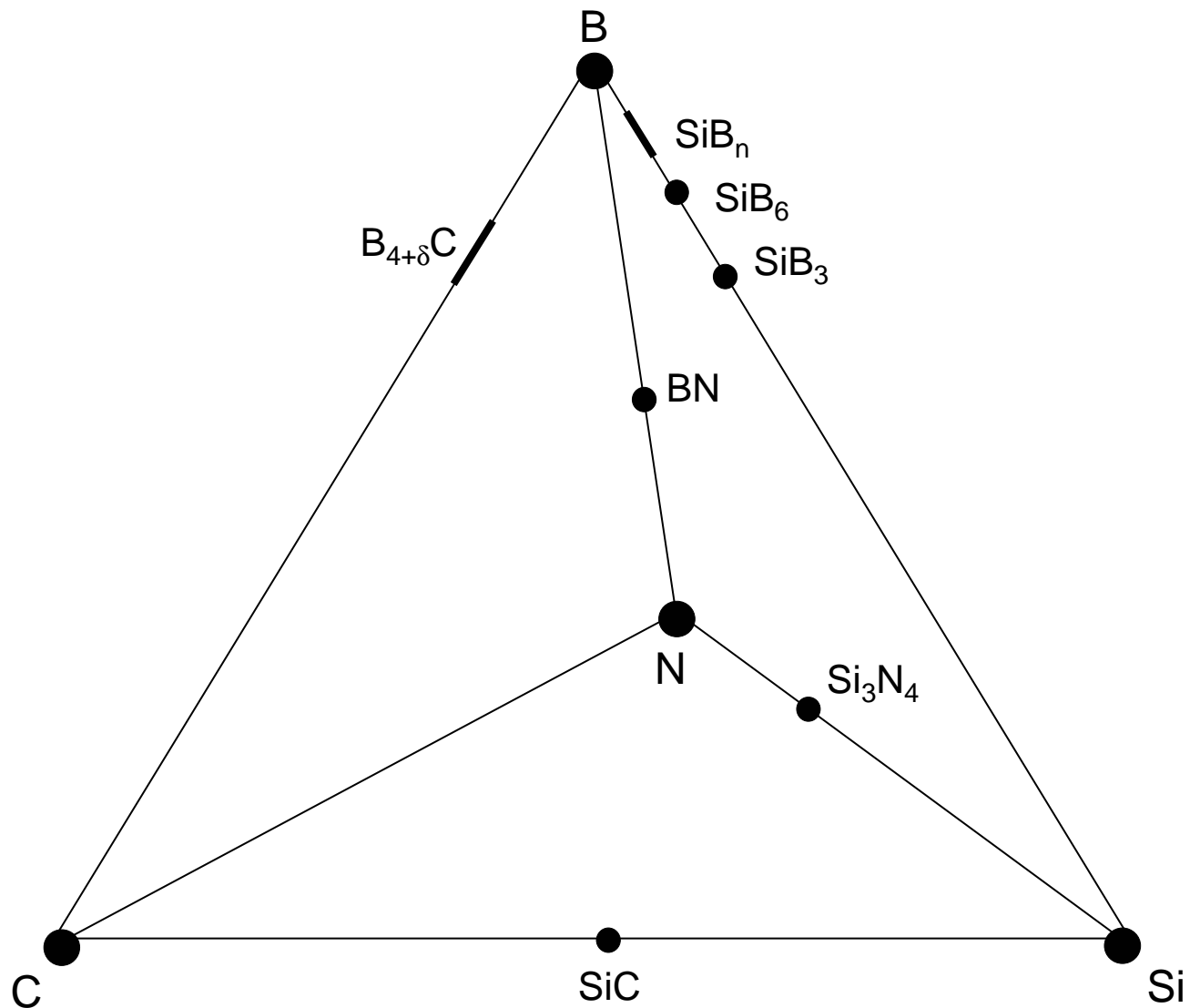
Calculated Phase Fraction Diagram of T2-1- Derived Ceramic $\text{Si}_{3.0}\text{B}_{1.0}\text{C}_{4.3}\text{N}_{2.0}$



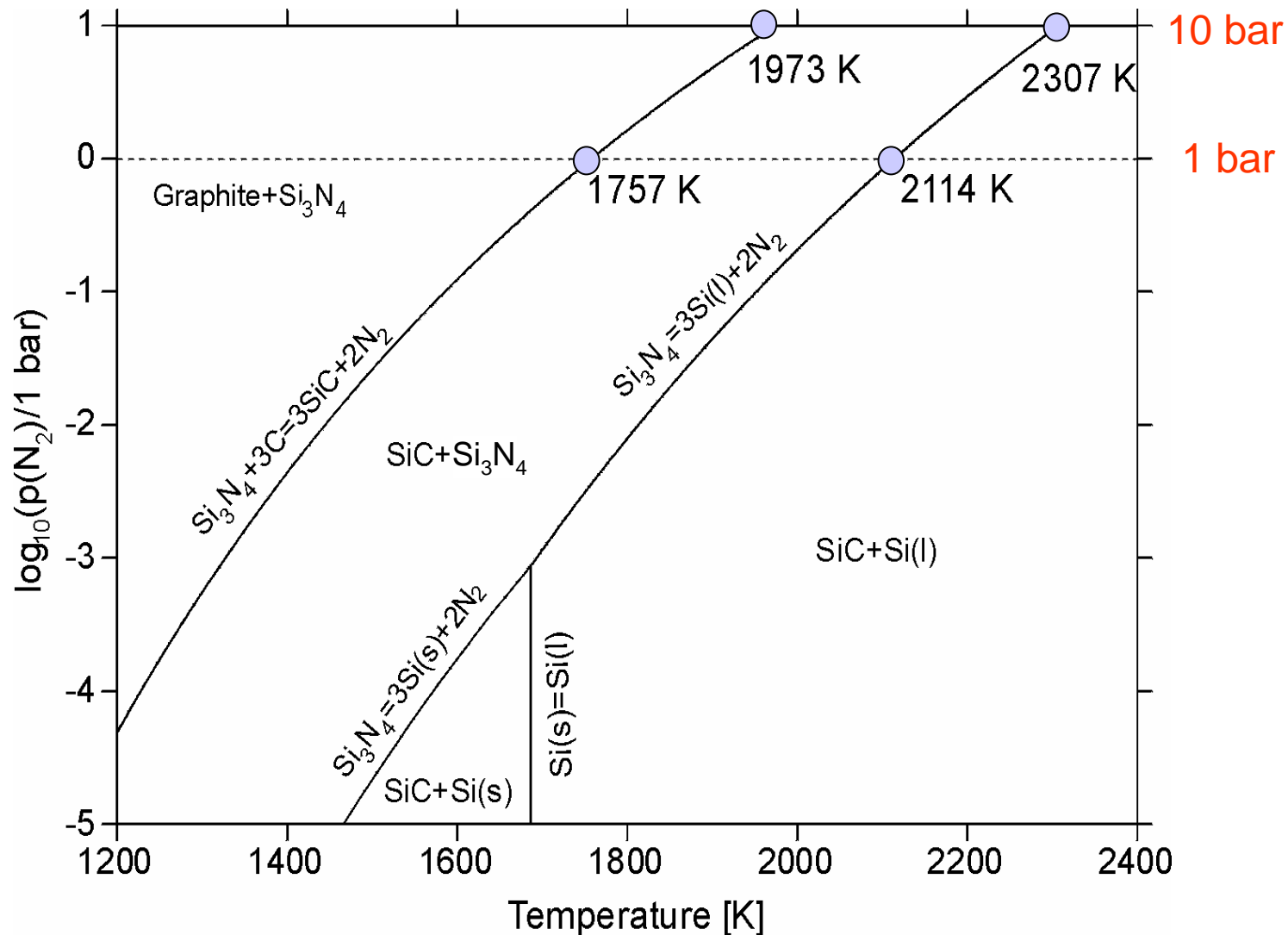


Isothermal Section at 1500 K in the Ternary System Si-B-C

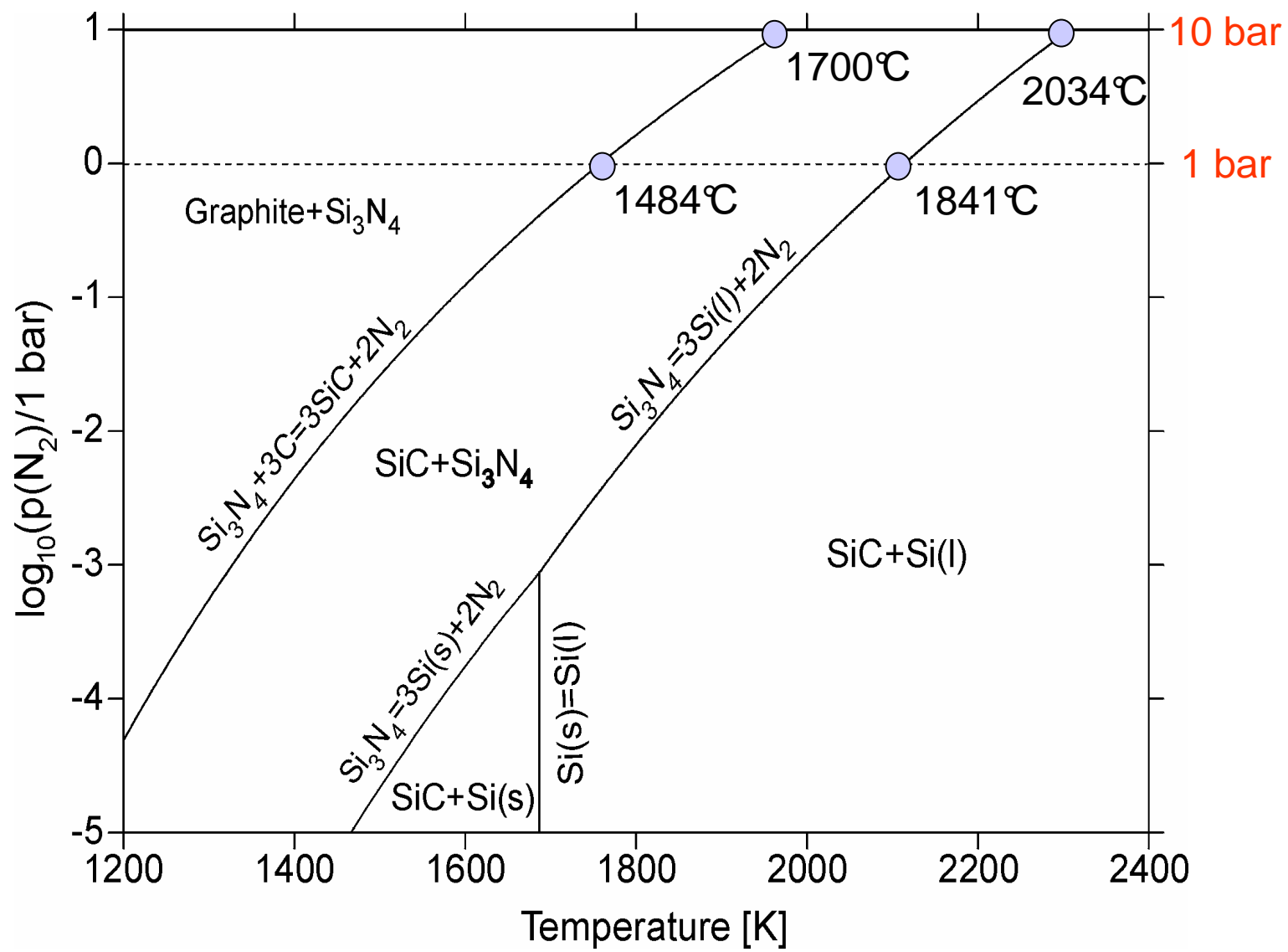




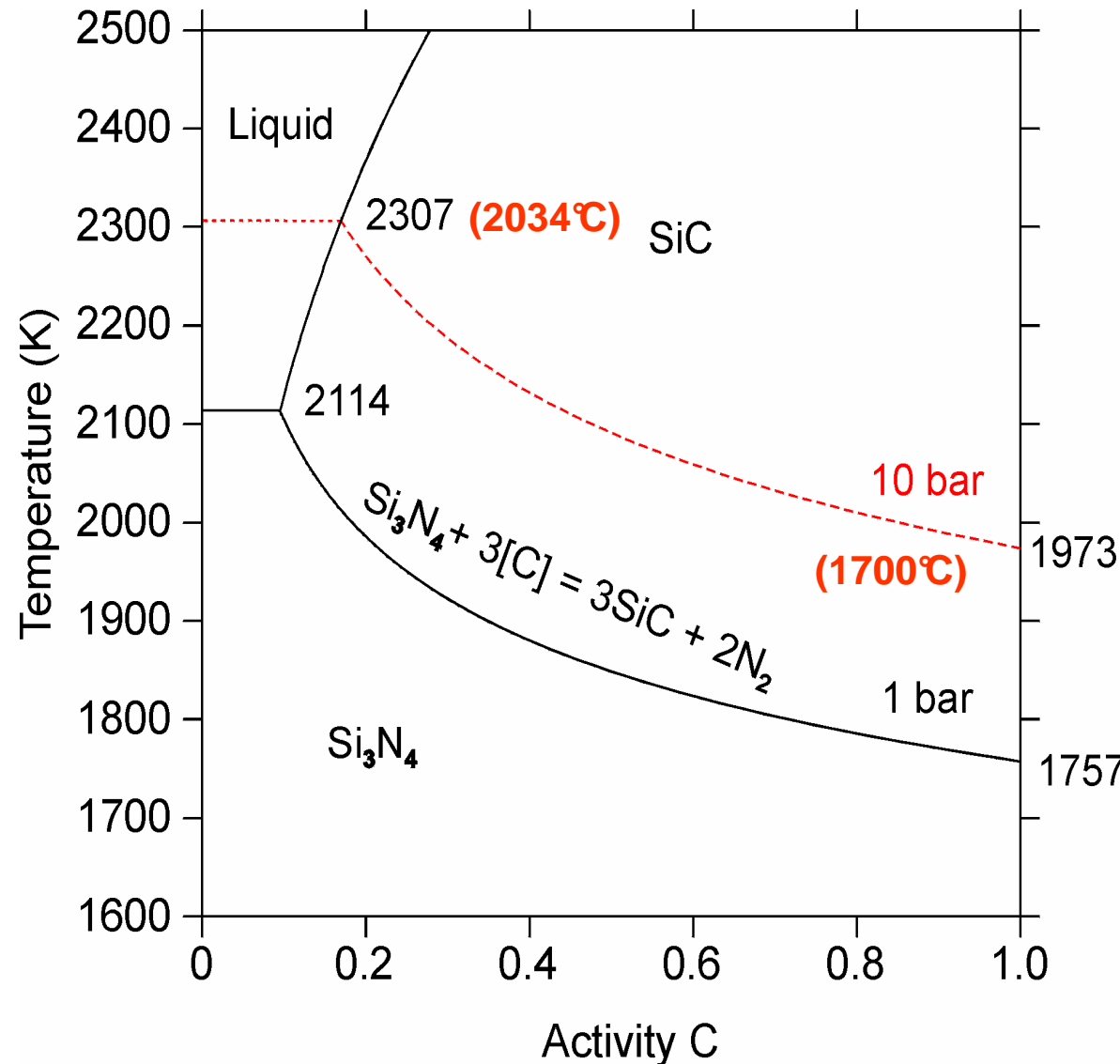
Calculated Potential Phase Diagram



Calculated Potential Phase Diagram



Carbon activity - temperature diagram

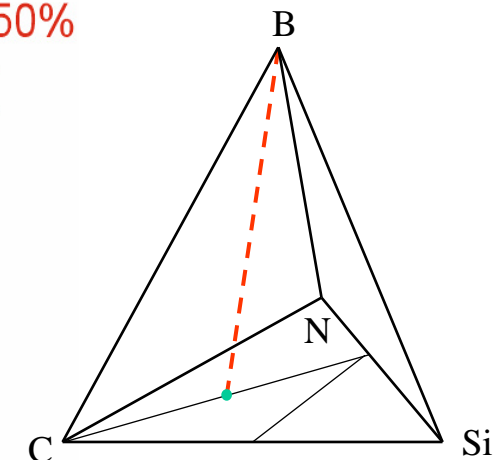
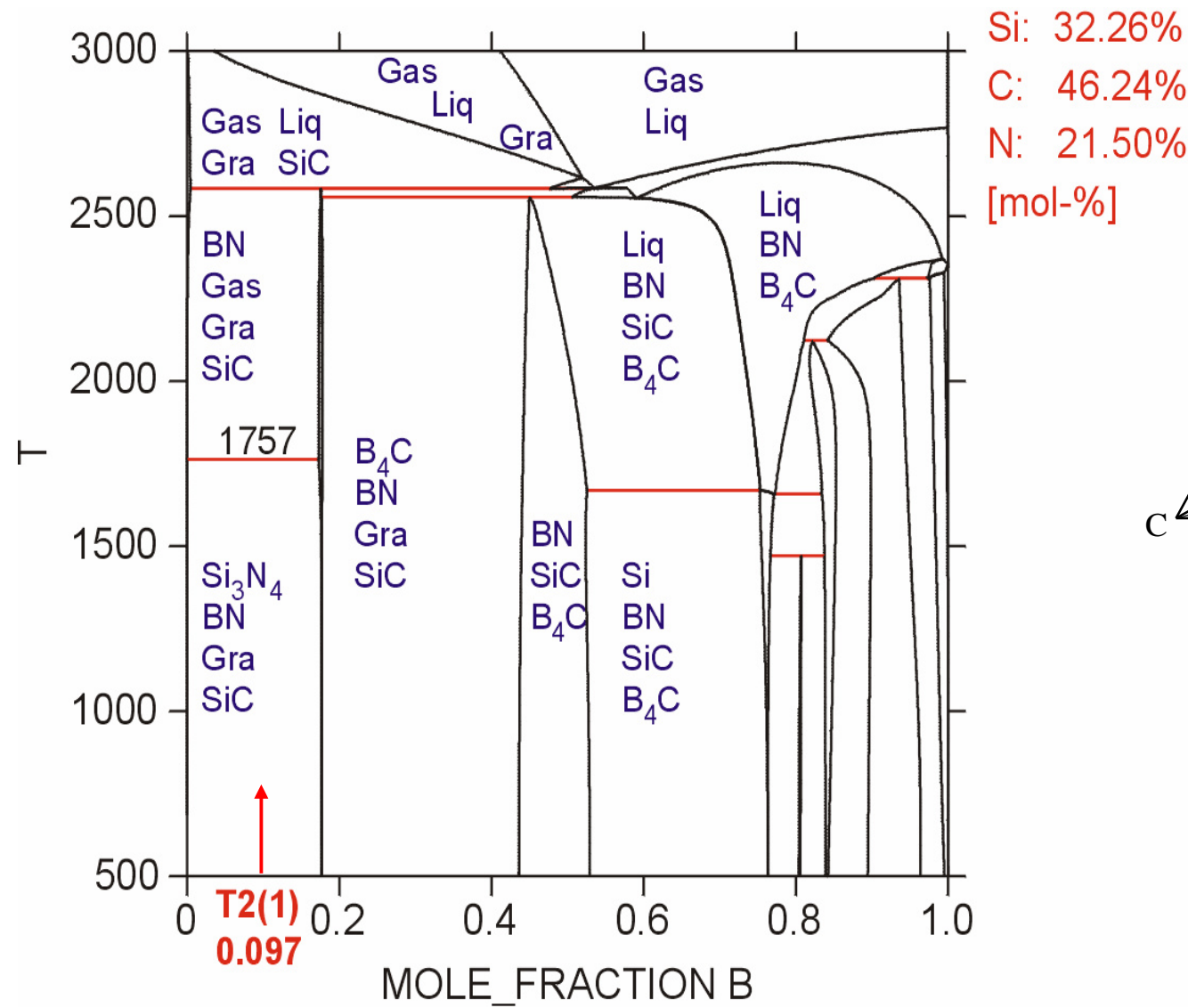


10 bar pressure:

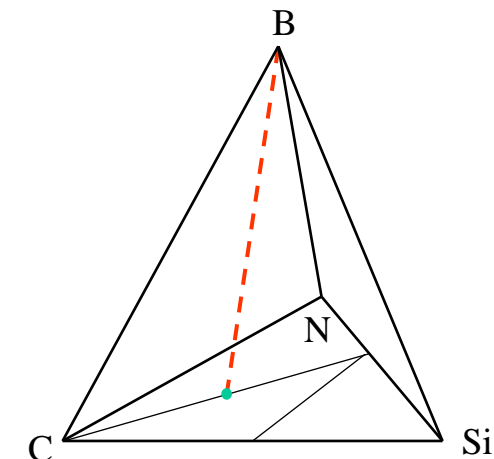
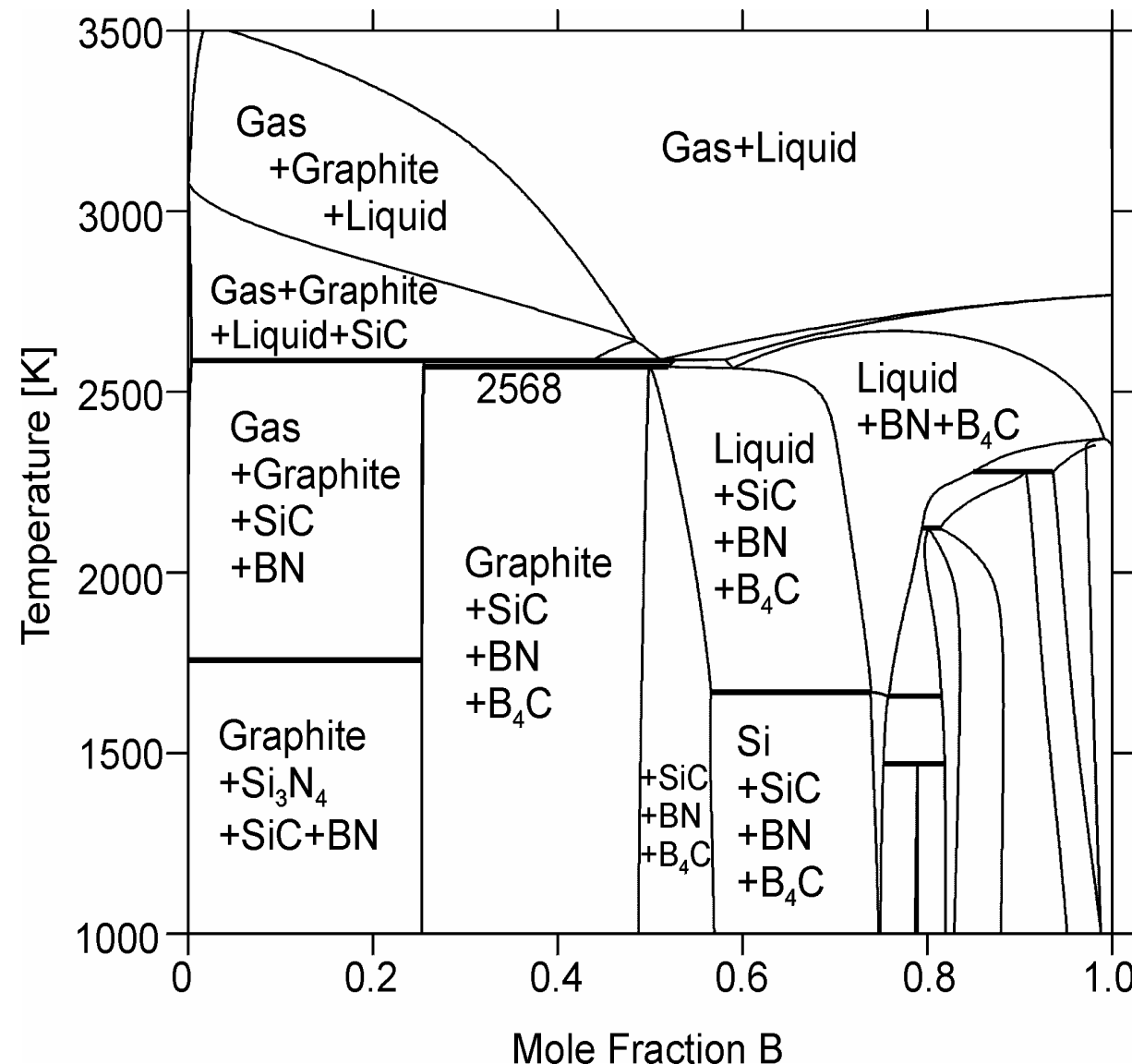
ac. = 1 1973 K (1700°C)

ac. = 0.17 2307 K (2034°)

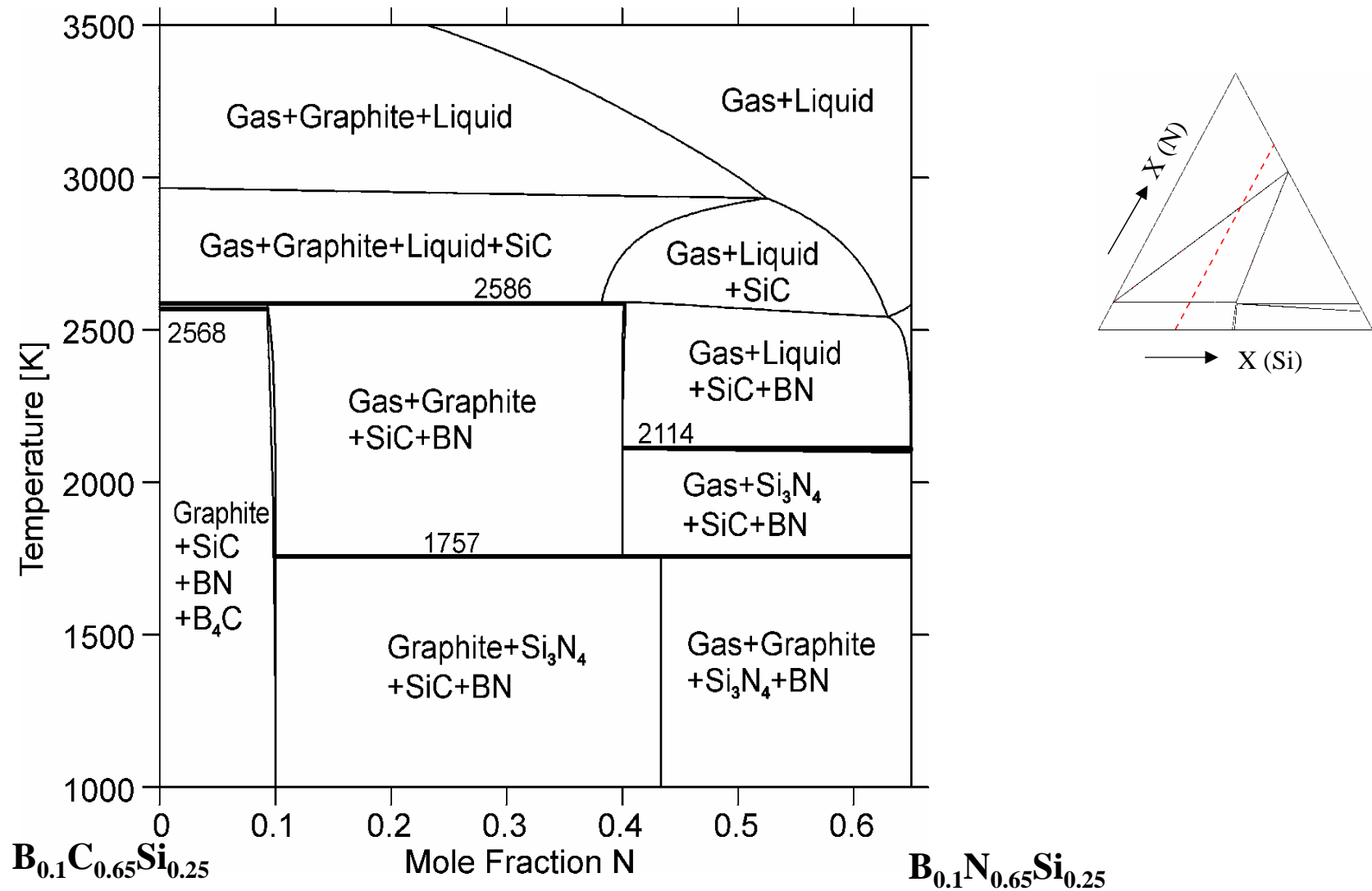
Estimating a pressure of 10 bar and a carbon activity of 0.17, it can be concluded that the thermal stability of precursor-derived Si-B-C-N ceramics remains up to 2000°C.

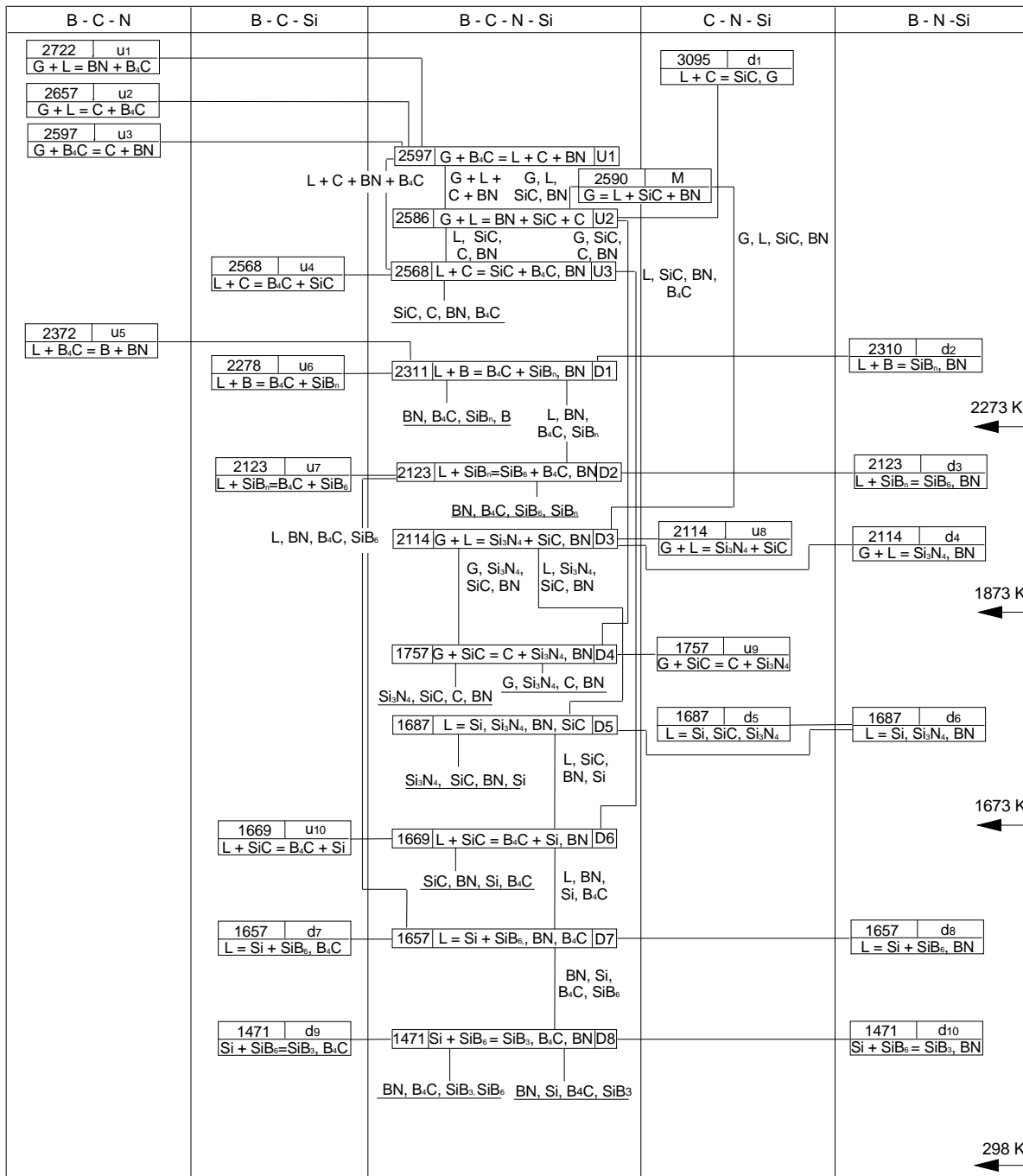


Isopleth from B to $\text{Si}_1\text{C}_{1.6}\text{N}_{1.33}$ (VT50) in the Si-B-C-N System

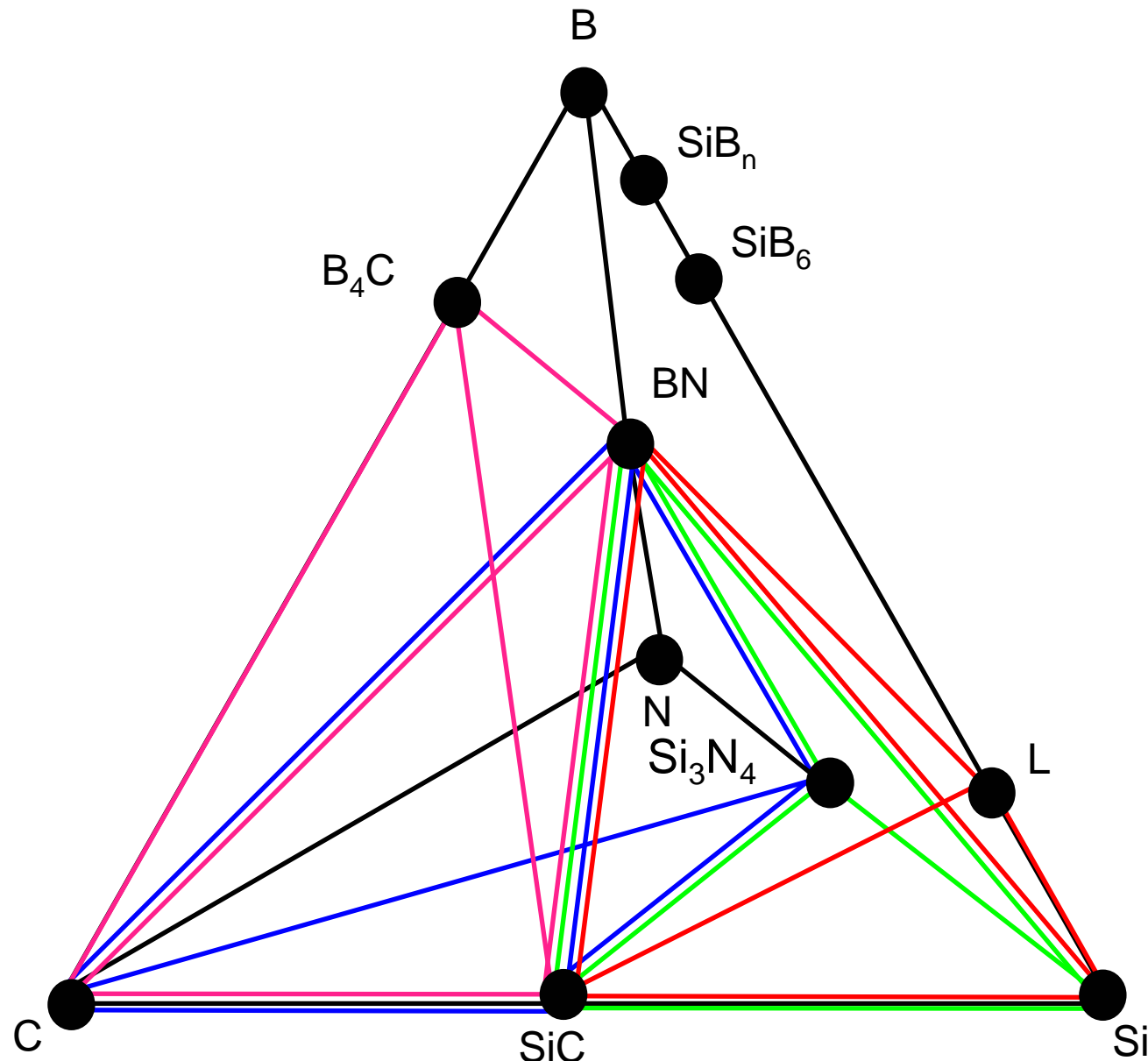


Isopleth from $B_{0.1}C_{0.65}Si_{0.25}$ to $B_{0.1}N_{0.65}Si_{0.25}$ in the Si-B-C-N System
 (at 10 mol-% B and 25 mol-% Si)

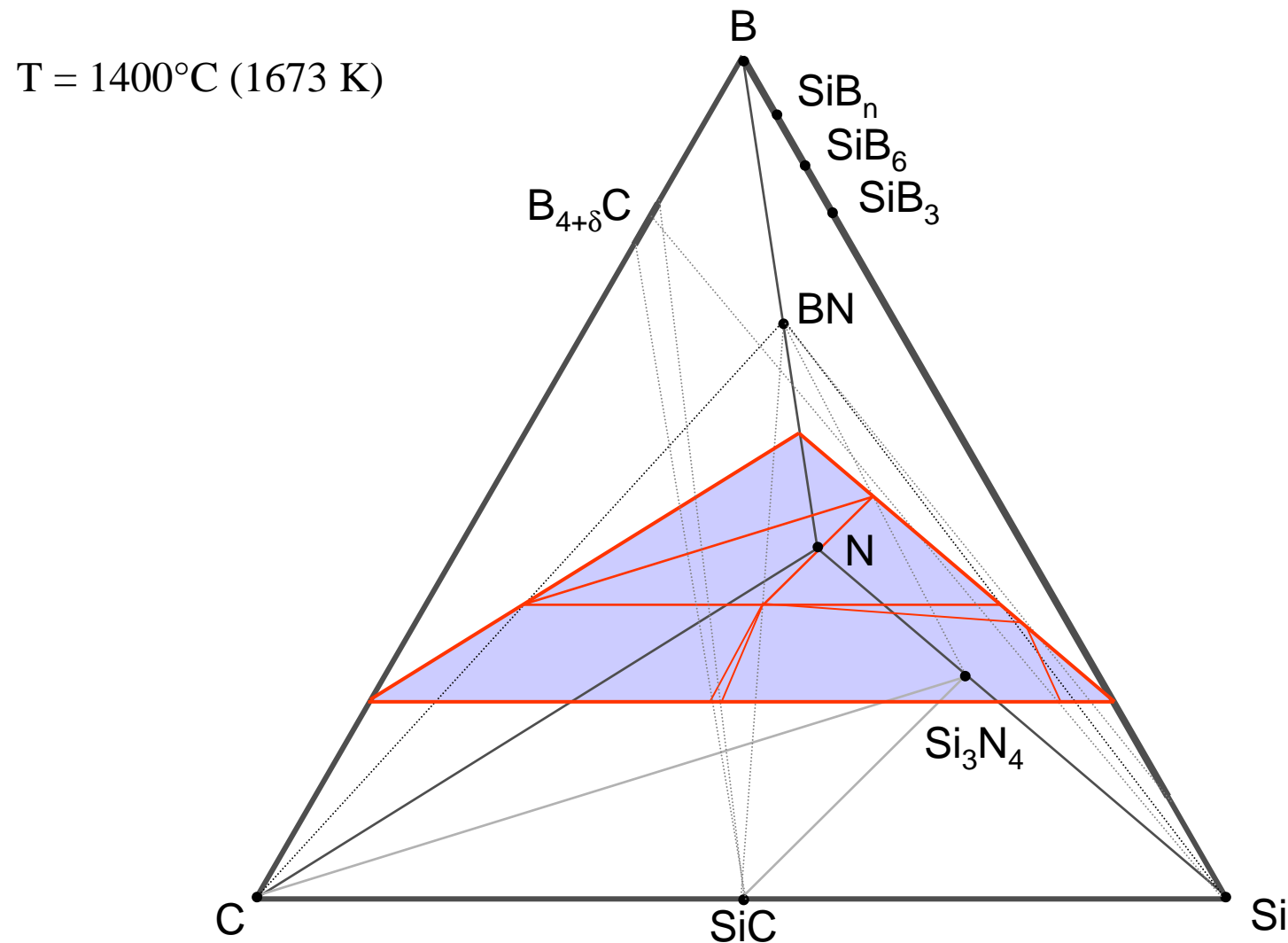




Si-B-C-N phase diagram at 1673 K with 4 of 9 4-phase equilibria

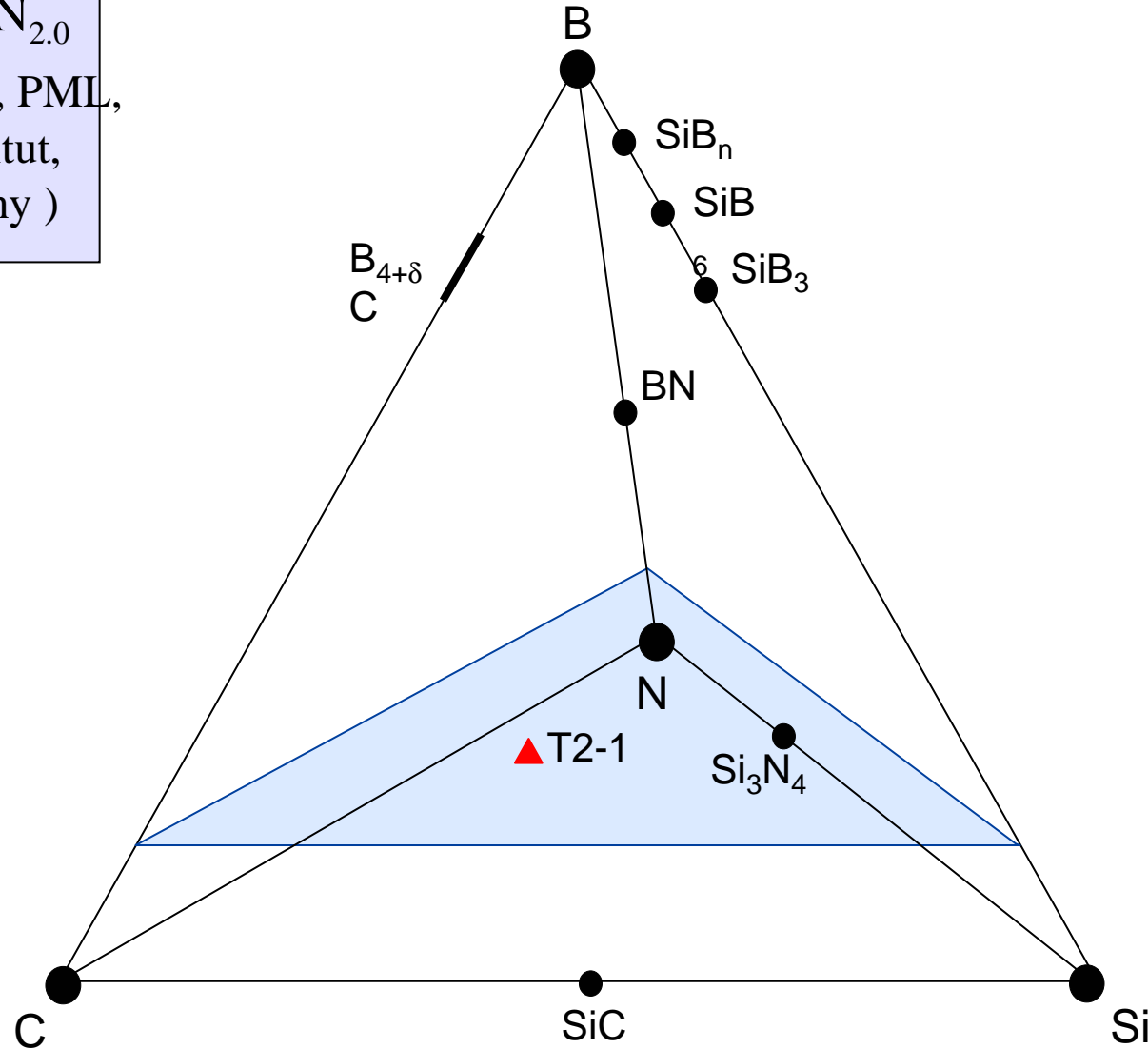


Si-B-C-N concentration tetrahedron with indicated
plane at a constant B content of 25 at.%

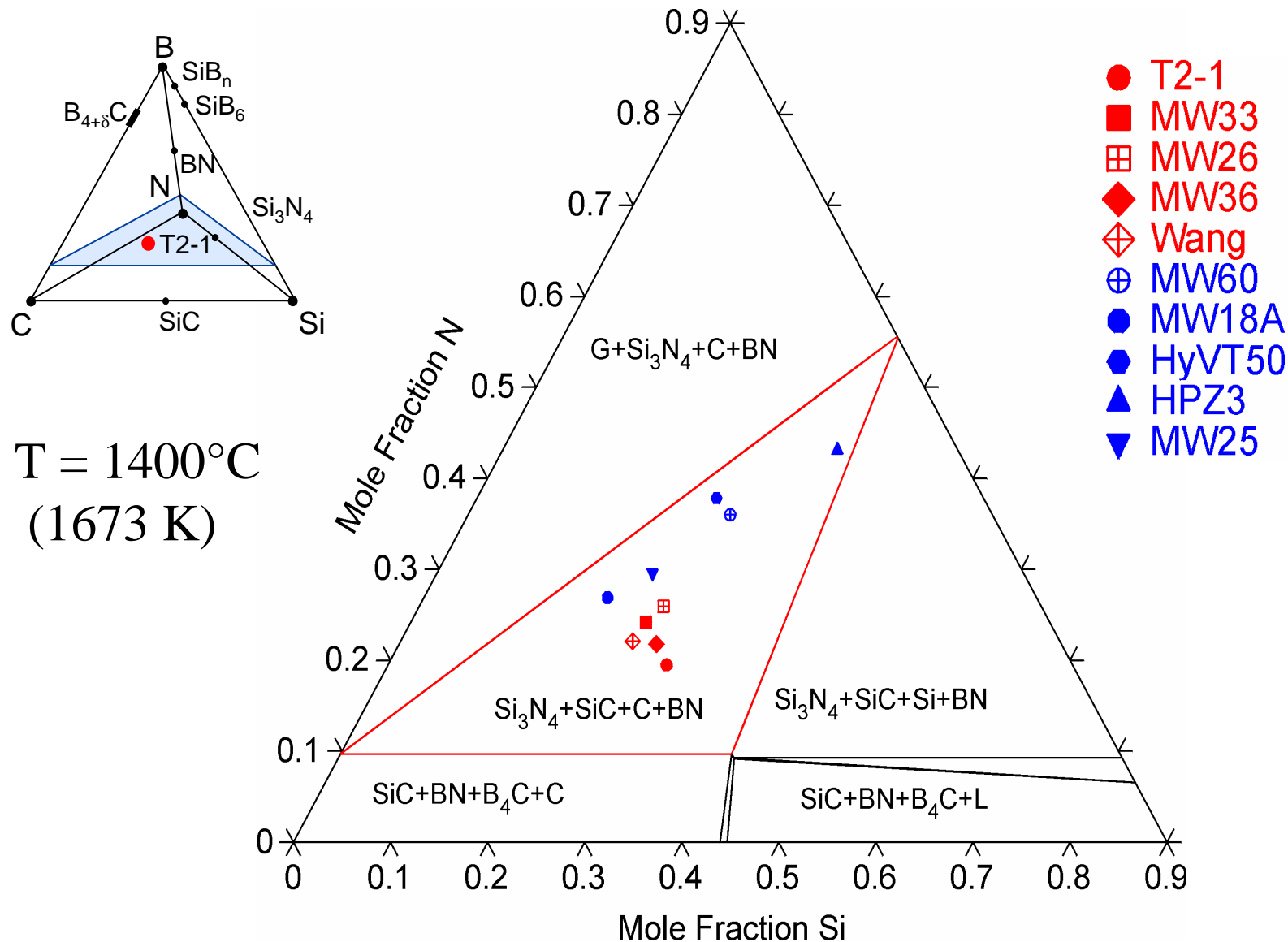


Si-B-C-N concentration tetrahedron with indicated plane at a constant B content of 10 at.%

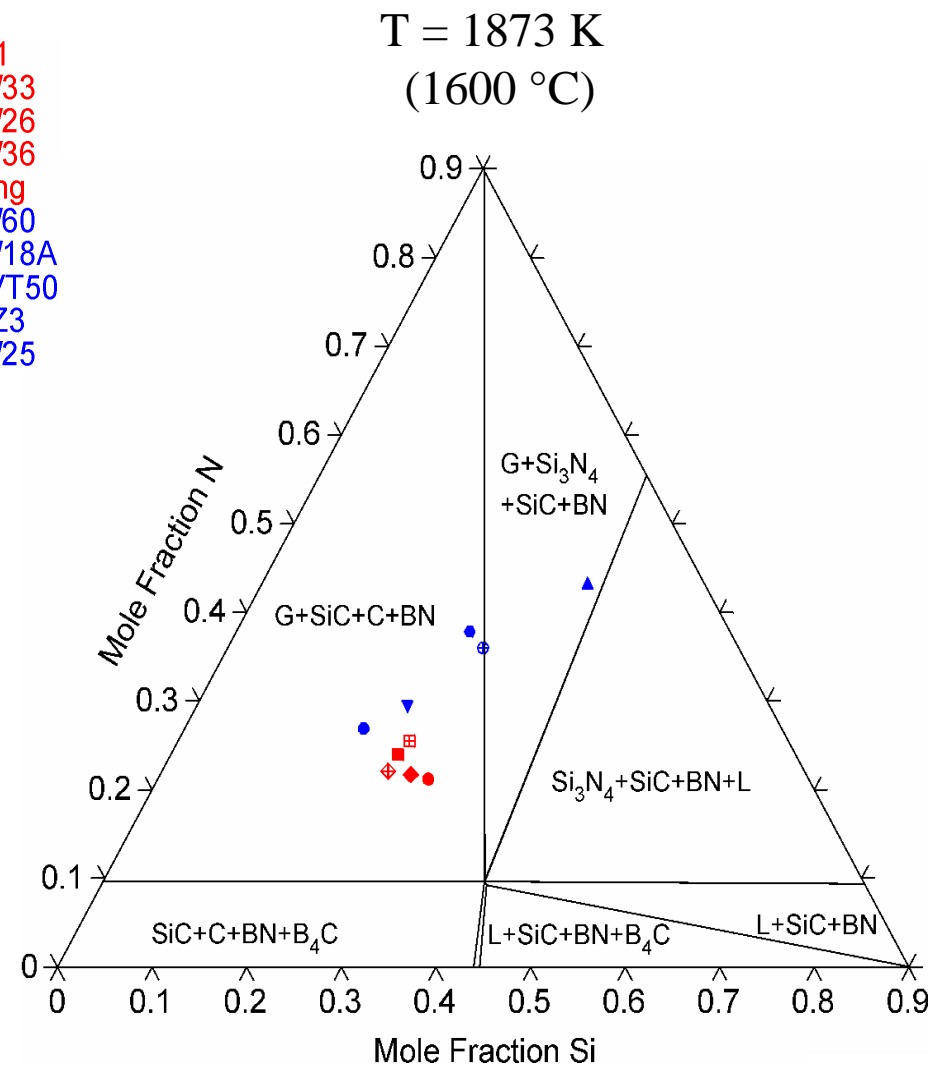
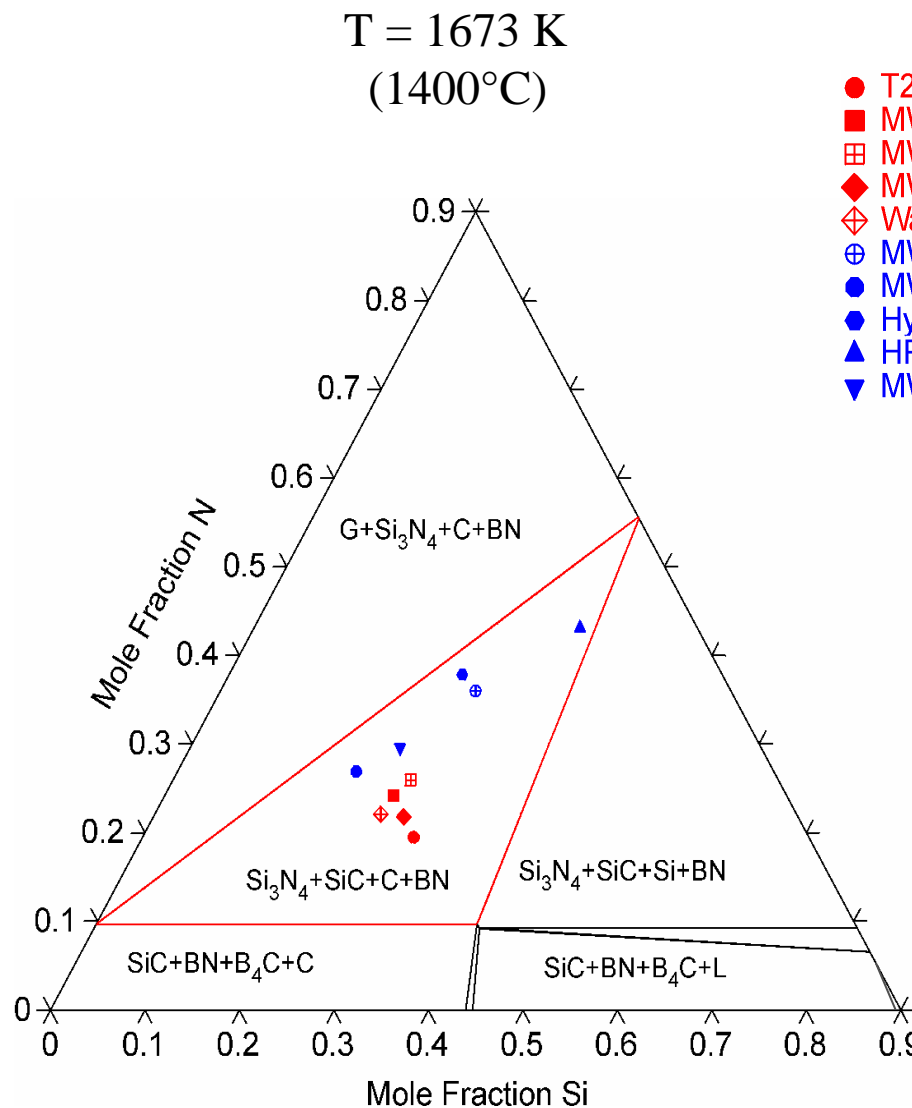
▲ $\text{Si}_{3.0}\text{B}_{1.0}\text{C}_{4.3}\text{N}_{2.0}$
(T2-1 precursor, PML,
Max-Planck-Institut,
Stuttgart, Germany)



Isothermal Section at 10 mol-% B in the Si-B-C-N System



Isothermal Sections at 10 mol-% B in the Si-B-C-N System



System Si-B-C-N

- Metastable phase separation -

